

DEPARTMENT OF METEOROLOGY
University of Helsinki
Report No. 50

THE SCAVENGING OF AIR POLLUTANTS BY
PRECIPITATION, AND ITS ESTIMATION WITH THE AID OF
WEATHER RADAR

by

Kirsti Jylhä

ACADEMIC DISSERTATION

To be presented, with the permission of the Faculty of Science of the
University of Helsinki, for public criticism in Auditorium XII,
Unioninkatu 34, on 8 December 2000 at 12 o'clock a.m.

Helsinki 2000

Helsingin yliopisto
Meteorologian laitos

Department of Meteorology
P.O.Box 4 (Yliopistonkatu 3)
FIN-00014 University of Helsinki
FINLAND

ISBN 951-45-9606-4 (printed version)

ISBN 951-45-9607-2 (pdf-version)

ISSN 0356-6897

Abstract

Precipitation cleanses the air by capturing airborne pollutants and depositing them onto the ground. The efficiency of this process may be expressed by the fractional depletion rate of pollutant concentrations in the air, designated as the scavenging coefficient Λ (s^{-1}). It depends on the size distribution of the raindrops and snow crystals and is thereby related to the precipitation rate R (mm h^{-1}) and the radar reflectivity factor Z ($\text{mm}^6 \text{m}^{-3}$). On the other hand, there are no universal $\Lambda - R$ and $\Lambda - Z$ relationships; these vary depending on the properties of the precipitation and pollutants. In this study, a few estimates for them were derived theoretically and empirically, using in the latter case observations made either after the Chernobyl nuclear accident or during a wintertime case study near the Inkoo coal-fired power plant.

For pollutants already incorporated into cloud droplets, a theoretical relation $\Lambda \approx 1.5 \cdot 10^{-5} \text{ s}^{-1} Z^{0.53}$ was obtained. This $\Lambda - Z$ relation, as well as the corresponding formula for below-cloud submicron aerosol particles and highly soluble gases, imply that in rain an increase of Z by a factor of 10 approximately corresponds to a two- to fourfold increase in Λ . The relation was supported by analysis of the Chernobyl data set. On the basis of the same data, the average scavenging coefficient for the particle-bound radionuclides involved was $\Lambda = (8 \mp 2) \cdot 10^{-5} \text{ s}^{-1} R^{0.65 \mp 0.02}$. This $\Lambda - R$ relation parameterised scavenging of long-range transported aerosol particles by hydrometeors mostly in the liquid phase. The Inkoo data set, when combined with modelling, suggested in turn that if $b=0.7$, then $\Lambda \leq 10^{-6} \text{ s}^{-1} R^b$ for sulphur emissions in wet snowfall within the first 10 km of the source. Because of the small spatial scale considered in that study, the model took into account the inclined fall trajectories of snowflakes through the plume.

The greatest advantage in the use of weather radar in assessing precipitation scavenging arises from the fact that radar estimates the spatial distributions of Z and, with certain assumptions, of R in real time with a good spatial and temporal resolution. In addition to their value in scientific research, radar measurements may also be utilized in emergency situations to make short-term forecasts of those areas most likely to be exposed to wet deposition.

Contents

1	Introduction	7
2	Theoretical background	10
2.1	Precipitation scavenging of aerosol particles	10
2.1.1	Nucleation scavenging	10
2.1.2	Impaction scavenging	11
2.2	Precipitation scavenging of gases	14
2.3	Precipitation scavenging of contaminated cloud particles	16
2.4	The scavenging coefficient and related parameters	18
2.5	The radar reflectivity factor	19
3	Methods and material	21
3.1	Basis for the $\Lambda - R$ and $\Lambda - Z$ relations	21
3.1.1	Irreversible below-cloud scavenging	21
3.1.2	In-cloud scavenging	24
3.2	Wet deposition on the ground	25
3.3	Observations	26
3.3.1	Data for studies related to the Chernobyl power plant	26
3.3.2	Data for studies related to the Inkoo power plant	27
3.4	Procedures	28
4	Results and discussion	29
4.1	The $\Lambda - R$ relationship	29
4.1.1	Results of studies related to the Chernobyl power plant	29
4.1.2	Results of studies related to the Inkoo power plant	33
4.2	The $\Lambda - Z$ relationship	36
4.2.1	Theoretical dependencies	36
4.2.2	An example related to Chernobyl	41
4.3	The use of weather radar in wet deposition estimates	43
4.3.1	General aspects	43
4.3.2	Remarks about the present studies	46
5	Summary	48
	Acknowledgements	50
	References	52
A	Corrections to Papers I and II	

1 Introduction

Nearly two-thirds of the electricity supply in the world is produced at fossil fuel power plants and about a quarter at nuclear power plants (IEA 1998; IAEA 2000). Electricity generation and other forms of fossil fuel consumption emit a large number of chemical species into the atmosphere, including oxides of carbon, sulphur and nitrogen (CO_2 , SO_2 , NO_x), hydrocarbons and particulate matter. Despite the fact that anthropogenic sulphur and nitrogen emissions into the air have started to decline in Europe (Berge et al. 1999) and North America (EPA 1998), on a global scale they may well increase during the next 20-50 years (Galloway 1995; IPCC 2000), largely because of the intensifying use of fossil fuels in eastern and southern Asia (e.g., van Aardenne et al. 1999; Streets et al. 1999). Emissions from nuclear power plants into the atmosphere are normally minor, but there is a risk of uncontrolled releases of radioactive materials into the air, as have occurred at Three Mile Island in Pennsylvania in 1979 and, particularly, at Chernobyl in the Ukraine in 1986. In addition to emissions connected with electricity production, radioactive materials may also be accidentally released into the air by, for example, the nuclear weapons industry and nuclear fuel-processing plants, as happened at Sellafield in England in 1957, at Kyshtym in the South Urals in 1957 and at Tokai-mura in Japan in 1999.

Materials emitted into the atmosphere are transported and mixed by airstreams, undergo chemical and physical transformation and are finally removed from the atmosphere by wet and dry deposition. Increased concentrations of many primary and secondary pollutants in the air constitute hazards to the health of human beings and animals. After being deposited onto the surface of the Earth they may cause, or contribute to, acidification, eutrophication or radioactive contamination of aquatic and terrestrial ecosystems, and thereby have both acute and chronic impacts on biological populations, as well as socio-economic effects on human societies (e.g., Rodhe et al. 1995; Savchenko 1995; González 1996; Appleby 1998; BASYS 2000). On the other hand, sulphate and nitrate aerosol particles, deriving from SO_2 and NO_x , may moderate global warming induced by anthropogenic emissions of CO_2 and other greenhouse gases (e.g., Roeckner et al. 1999; Toon 2000).

After the Chernobyl nuclear accident, the need to improve early warning procedures for radioactive fallout was clearly realized. Since that time, strategies for monitoring, assessing and decision-making in an emergency have been under further development (e.g., Weiss 1997), involving also the evolution of operational real-time dispersion models (e.g., Saltbones et al. 1998; Langner et al. 1998). In the Chernobyl case, the radiation fallout patterns were typically linked with precipitation fields (e.g., Savolainen et al. 1986; Pers-

son et al. 1987; Wernli 1987; Clark and Smith 1988; Erlandsson and Isaksson 1988; Arvela et al. 1990; Puhakka et al. 1990; Hirose et al. 1993; Paatero 2000) which indicates the importance of precipitation in depositing radioactive materials onto the ground. For modelling wet deposition, it is therefore necessary to appraise three elements: the dispersion of the air pollutants, the occurrence of precipitation on the track of the air pollutants, and the efficiency with which the precipitation scavenges them. Obviously, this threefold problem has to be solved not only in the case of radioactive pollutants, but also for other harmful substances in the air.

This doctoral dissertation concerns itself with the scavenging of air pollutants by precipitation and the estimation of such scavenging with the aid of weather radar. Precipitation scavenging includes in-cloud and below-cloud processes whereby pollutants become attached to liquid or solid hydrometeors, followed by the fall of the hydrometeors to the ground as rain or snow. The development of radar (RAdio Detection And Ranging) in 1920-1950 was primarily driven by military needs (Skolnik 1962, p. 11), but after World War II radars also found many civilian applications, including the remote sensing of precipitation. Precipitation measurements by weather radar are conventionally utilised by meteorologists and hydrologists; however, they may also be profitable in radioactivity protection activities and wet deposition research. This potential of weather radar measurements has previously been considered or utilised, or both, by e.g. Smith (1981), ApSimon et al. (1988), Puhakka et al. (1990), Goddard and Conway (1990), Savolainen et al. (1991) and Dvonch et al. (1998), along with Jylhä et al. (1986) and Jylhä (1989). In the following, the issue is further deliberated on the basis of five papers, hereafter referred to by their corresponding Roman numerals:

- I Jylhä, K., 1991: Empirical scavenging coefficients of radioactive substances released from Chernobyl. *Atmos. Environ.*, 25A, 263–270.
- II Jylhä, K., 1999a: Relationship between the scavenging coefficient for pollutants in precipitation and the radar reflectivity factor. Part I: Derivation. *J. Appl. Meteor.*, 38, 1421–1434.
- III Jylhä, K., 1999b: Relationship between the scavenging coefficient for pollutants in precipitation and the radar reflectivity factor. Part II: Applications. *J. Appl. Meteor.*, 38, 1435–1447.
- IV Jylhä, K., 1995: Deposition around a coal-fired power station during a wintertime precipitation event. *Water, Air, Soil Pollut.*, 85, 2125–2130.
- V Jylhä, K., 2000: Removal by snowfall of emissions from a coal-fired power station: observations and modelling. *Water, Air, Soil Pollut.*, 120, 397–420.

Paper I is an experimental study of the scavenging of aerosol particles by precipitation. It is based on weather radar and radioactivity measurements after the Chernobyl accident, and resulted in an empirical relationship between the intensity R (mm h^{-1}) of precipitation and its efficiency in removing pollutants from the atmosphere. This efficiency is described by the fractional depletion rate of the pollutant concentration in air due to scavenging, known as the precipitation scavenging coefficient Λ (s^{-1}) and first discussed in the 1950's and 1960's by e.g., Chamberlain (1959), Makhon'ko and Malakhov (1967) and Engelmann (1968). Papers II and III likewise deal with Λ , but instead of using a $\Lambda - R$ relation, they propose an alternative method to utilise weather radar measurements in estimates of Λ . The method is based on the fact that, like Λ and R , the primary quantity in radar meteorology, the so-called radar reflectivity factor Z ($\text{mm}^6 \text{m}^{-3}$), is also a function of the hydrometeor size distribution. The theoretical basis of the $\Lambda - Z$ relation and factors affecting its form are considered in II, and III deliberates its use to provide a first estimate of wet deposition; a demonstration related to the Chernobyl accident is also given.

An estimate for the uppermost limit of Λ for freshly-emitted sulphur in snowfall is obtained in Paper V. The experiment discussed in that paper and in the accompanying Paper IV was carried out at Inkoo on the south coast of Finland in order to explore the influence of a 250 MW coal-fired power plant unit on ambient air concentrations and on deposition. While the measurement procedure, the weather situation and the chemical analysis results are documented in detail in Jylhä (1996), the main objectives of Papers IV and V are to find, with the aid of modelling, possible explanations for the observations. In addition, an essential goal of V is to roughly estimate the scavenging efficiency of snowfall at temperatures close to 0°C . Slightly different parameterisations are used in the model estimates of IV and V, the consequences of which are also referred to in V.

This summary starts with a theoretical review of precipitation scavenging that is to a large extent based on the text books by Pruppacher and Klett (1997) and Seinfeld and Pandis (1998), referred to in the following as PK (1997) and SP (1998), respectively. It then gives the basic features of weather radar and discusses the more essential formulas used in I-V. The observational data sets and methods used are shortly introduced, after which the main results of I-V are considered.

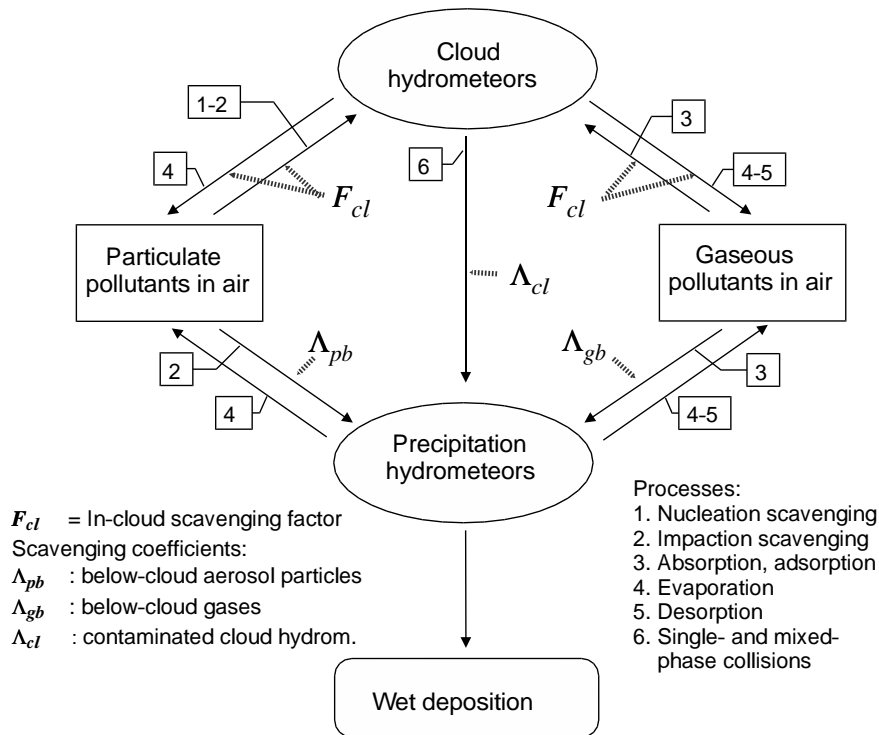


Fig. 1 Interaction diagram of wet deposition processes and the parameters used to describe them.

2 Theoretical background

2.1 Precipitation scavenging of aerosol particles

Atmospheric aerosol particles (APs) are incorporated into hydrometeors by several mechanisms that can be separated into two groups: nucleation scavenging and impaction scavenging (Fig. 1). In nucleation scavenging APs serve as cloud condensation or ice-forming nuclei in the initial phase of hydrometeor formation, whereas in impaction scavenging they collide with and stick to existing cloud droplets, raindrops or snow crystals. Nucleation scavenging is controlled by the requirements for heterogeneous nucleation in the atmosphere. Impaction scavenging depends, in turn, on the net action of various forces influencing the relative motion of APs and hydrometeors.

2.1.1 Nucleation scavenging

At the beginning of cloud formation nucleation scavenging entirely dominates impaction scavenging. Both experimental and theoretical investigations indicate that it may deplete the original AP population in the air by up to 75-90% or even more, depending on the

sizes and chemical composition of the APs and on ambient conditions (PK 1997, p. 716-719). Ignoring here haze and fog condensation (e.g., PK 1997, p. 13, 173; SP 1998, p. 1047; Laaksonen et al. 1998), a necessary requirement for nucleation scavenging is the supersaturation of the air containing APs. This demand is usually met as a result of the cooling of air during its ascent or its transfer to a colder region. The higher the supersaturation and the larger the water-soluble fraction and hygroscopicity of APs, the smaller are those APs which become activated to grow into cloud droplets (e.g., PK 1997, p. 175-178, Korhonen et al. 1996; Eichel et al. 1996). On the other hand, large and wettable but water-insoluble APs, such as combustion and desert particles, may also be subject to scavenging by drop nucleation. In this case, adsorption of water vapour and subsequent condensation occur preferentially at particular active sites which differ morphologically, chemically or electrically from the rest of the surface material of the APs (PK 1997, p. 297-308).

If a critical ice supersaturation is exceeded, the inhomogeneity locations on water-insoluble APs may also serve as active sites to ice nucleation in the deposition mode (PK 1997, p. 330-338). In general, ice-forming nuclei are highly water-insoluble and have chemical bonding and crystallographic structures similar to ice. However, little is known as to how significant the active sites on the surface of APs are to the other modes of ice nucleation, referred to as the freezing, immersion and contact modes (PK 1997, p. 309, 326-341; SP 1998, p. 827). These three ice nucleation modes are preceded by interaction between APs and liquid droplets; only during or after the capture of ice-forming nuclei will freezing of the droplets take place. As shown by Respondek et al. (1995), the presence of an ice phase in mixed ice-water clouds significantly affects wet deposition onto the ground. In spite of that, and although ice nucleation dominates impaction scavenging of inactivated APs by ice crystals, it can be neglected in comparison to drop nucleation scavenging (Alheit et al. 1990).

2.1.2 Impaction scavenging

A fraction of those APs that remain unscavenged by nucleation may subsequently be incorporated into cloud and precipitation hydrometeors through impaction scavenging (Fig. 1). Potential mechanisms are convective Brownian diffusion, interception, inertial impaction, thermophoresis, diffusiophoresis, airflow turbulence, and electrostatic attraction (e.g., Hinds 1982, p. 174-178; PK 1997, p. 720-744, 846-852). These mechanisms involve different kinds of relative motions of APs and hydrometeors, which are basically governed by the principles of the conservation of mass, momentum and electric charge. Whether or not impaction scavenging of APs results from such motions strongly depends

on the characteristics of the APs, the hydrometeors and the viscous medium, the air.

Small APs with little inertia are exposed to scavenging by Brownian diffusion, since they are likely to undergo a net transport towards hydrometeors owing to their irregular motions induced by thermal bombardment by gas molecules. The fall of hydrometeors relative to such APs, or in other words, the convection of the APs relative to the hydrometeors, further enhances the probability of convective diffusional collisions. Large APs, on the other hand, tend to experience inertial impaction because they have too much inertia, as compared with the kinematic viscosity of the air, to be able to follow the abruptly-changing gas streamlines in the vicinity of hydrometeors. Instead, their inertia acts to keep them on a collision trajectory. If APs manage to follow the streamlines but still happen to graze the hydrometeors, interception occurs. Electrostatic attraction results in turn from oppositely-charged hydrometeors and APs. Thermophoresis is caused by uneven heating of APs in ambient temperature gradients, and drives APs towards evaporating and sublimating hydrometeors, which are colder than their surroundings. Diffusiophoretic scavenging has the opposite direction: it is related to concentration gradients in water vapour and moves APs towards diffusively-growing hydrometeors. Lastly, scavenging by turbulence ensues from relative motions between APs and hydrometeors that are produced by velocity gradients in turbulent air or by an uneven response of APs and hydrometeors to local turbulent accelerations.

The efficiency of a single hydrometeor in collecting APs is described by the so-called collection kernel K_p , i.e. the effective volume swept out by the hydrometeor in unit time (PK 1997, p. 570). When multiplied by the number of APs in a fixed size range per unit volume, K_p represents the number of those APs in that range which are collected by the hydrometeor in unit time due to the joint action of the various impaction mechanisms. It may be expressed as

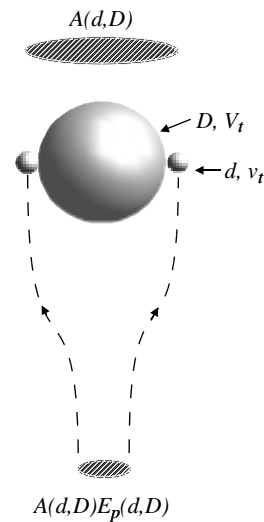
$$K_p(d, D) = A(d, D)|V_t(D) - v_t(d)|E_p(d, D) \quad (2.1)$$

where D , d , V_t and v_t are the diameters and fall speeds of the hydrometeor and the aerosol particles, respectively; $A(d, D)$ denotes the geometric cross-sectional area of a pair of impacting bodies oriented perpendicular to their fall direction (Fig. 2); $E_p(d, D)$ is the collection efficiency of the particles by the hydrometeor, defined to be the ratio of the actual cross-section for particle capture to the geometric cross-section $A(d, D)$ (e.g., PK 1997, p. 735).

When small APs collide with hydrometeors, they are likely to remain attached so that their collection efficiency $E_p(d, D)$ can be taken as equal to the collision efficiency (PK

1998, p. 592, 730). During their fall through air, large and irregular hydrometeors induce complicated flow fields around themselves. These fields influence collisions between APs and hydrometeors, but require rigorous methods and plenty of computer resources in order to be solved (PK 1997, p. 736; Wang and Ji 1997). However, if only hydrometeors with simple shapes and moderate sizes are considered, one can assume an axisymmetric flow around the interacting bodies. As reviewed by PK (1997, p. 732-739, 846-852), $E_p(d, D)$ can then be determined by a method having two modes, one for small APs ($d < 1 \mu\text{m}$) without inertial impaction, and the other for large APs ($d > 1 \mu\text{m}$) without Brownian diffusion. The method takes into account phoretic and electrostatic forces, too, and is applicable to spherical water drops and planar ice crystals smaller than about 1 mm, and to columnar ice crystals shorter than about 2.5 mm.

Fig. 2 Schematic presenting the relationship between the geometric cross-sectional area $A(d, D)$ and the collision efficiency of a tiny particle by a larger one; or assuming a sticking efficiency of unity, between $A(d, D)$ and the collection efficiency $E_p(d, D)$. Two grazing trajectories are also shown.



As summarized by PK (1997) and Wang and Lin (1995), the resulting values of $E_p(d, D)$ exhibit a minimum at intermediate AP sizes between about 0.01 and 1 μm , within the so-called Greenfield gap, where both Brownian diffusion and inertial impaction are ineffective. The exact depth, width and position of this minimum depend on the properties of the APs and hydrometeors, and on ambient conditions. In the case of subsaturation or electricity in clouds, the gap is partially filled owing to, respectively, phoretic and electrostatic attractions. The influence of subsaturation is associated with the direction of the net phoretic transfer (Martin et al. 1980). Within the Greenfield gap, thermophoresis dominates over diffusiphoresis, so that in the case of single-phase hydrometeors, phoretic scavenging becomes more efficient with decreasing relative humidity of air (with respect to either water or ice). However, in ice-water clouds and precipitation, the net phoretic transfer is directed away from ice crystals towards supercooled liquid drops. This adds to scavenging by drops but reduces scavenging by ice crystals. On the other hand, if the ice particles are not single compact crystals but porous snowflakes that permit

AP-containing air to flow through themselves, a filtering effect tends to partially fill the minimum in $E_p(d, D)$ (Mitra et al. 1990a).

Obviously, the collection kernel is not only a function of the collected particle size d but also varies with the collector particle size D . By combining the theoretical and experimental results of several authors, two typical dependencies of $E_p(d, D)$ on D may be found: either a monotonous decrease of $E_p(d, D)$ with increasing D (Sauter and Wang 1989; Miller and Wang 1989; Wang and Lin 1995), or a more complicated behaviour, with a decrease of $E_p(d, D)$ with D down to a local minimum, then an increase up to a local maximum near a hydrometeor size of 1 mm and finally a rapid decrease with further increasing D (Wang and Pruppacher 1977; Martin et al. 1980; Wang and Lin 1995). At the same time, however, the collection kernel $K_p(d, D)$ may increase, since the other relevant factors in (2.1), i.e., the fall speed difference $V_t - v_t$ and the cross-sectional area $A(d, D)$, increase with D .

Although APs within the Greenfield gap size range are poorly scavenged by impaction mechanisms, particularly in saturated air, they are typically those which most readily initiate drop formation in the atmosphere, and which are hence efficiently incorporated into cloud water (e.g., PK 1997, p. 744). Therefore APs in the Greenfield gap may also be deposited to the ground, provided that cloud formation is followed by precipitation. This issue will be deliberated later in Sec. 2.3.

2.2 Precipitation scavenging of gases

In analogy with the convective Brownian diffusion of APs, gas scavenging starts with diffusion of a gaseous species to the surface of hydrometeors. In the next stage, the gas molecules become dissolved in liquid drops or in a quasi-liquid layer at the surface of ice particles, after which some compounds, like SO_2 , NH_3 and HNO_3 , dissociate into ions. Alternatively, the gas is adsorbed onto solid ice surfaces (Fig. 1). The quasi-liquid layer on the ice surface refers to the presence of highly mobile water molecules at the ice-air interface. The mobility of the molecules increases with temperature, so that the layer is thickest at temperatures close to 0°C (PK 1997, p. 153-155). During the final stage of gas scavenging, gas molecules and ions diffuse inside liquid and solid hydrometeors, and may take part in chemical reactions (PK 1997, p. 155-157, 744-746, 783).

In general, absorption (and desorption) of a gas by a water drop is a coupled process between diffusion outside and inside the drop (PK 1997, p. 764-777; SP 1998, p. 607-616). However, if the aqueous-phase diffusion is rapid enough, so that the drop remains well-mixed practically all the time, with a nearly uniform species concentration inside it, the influence of aqueous-phase diffusion on gas scavenging can be ignored. In this case

the rate of gas absorption (or desorption) by a drop of diameter D , normalised by the ambient gas-phase concentration c_g , may be written as

$$J_n(D) = 2\pi D d_g f_v (1 - c_{gs}/c_g) \quad (2.2)$$

where d_g is the molecular diffusivity of the species in air ($\text{m}^2 \text{s}^{-1}$) and c_{gs} is the gas-phase concentration at the droplet surface, to be discussed below (PK 1997, p. 761-763; SP 1998, p. 597, 1003). The ventilation factor f_v is a dimensionless quantity (≥ 1) which describes the convective enhancement of diffusion due to the fact that falling hydrometeors strengthen relative motions between themselves and gas molecules (PK 1997, p. 537, 762). For a given species in the air, f_v is a function of D , V_t , d_g and the kinematic viscosity ν of the air (see Paper II for details).

Equation (2.2) states that the drop's capacity for receiving and holding the gas strongly depends on the difference between the concentrations in the ambient air and on the drop surface. The latter concentration decreases with an increasing ability of the gas to be dissolved in water (e.g., PK 1997, p. 761). Hence for a very soluble species, such as HNO_3 , one may make the approximation $c_{gs} \approx 0$. In this case the gas uptake is an irreversible process without any desorption, and the drop involved acts as a perfect sink with an infinite capacity for absorbing the gas and a continuously increasing aqueous-phase concentration c_l inside it (PK 1997, p. 757-759; SP 1998, p. 1003-1005). On the other hand, for gases, such as SO_2 , having a moderate solubility in water, c_{gs} is nonzero but proportional to c_l . Therefore, as c_l increases with the time of exposure, the rate of the uptake of gas is rapid at first, gradually decreasing thereafter. Besides being such a self-limiting process, the scavenging of SO_2 is dependent on other species present and is a reversible process: if the drop is exposed to air in which $c_g < c_{gs}$, the gas is desorbed.

No theoretical formulations are available at present for the concentration c_{gs} of a gas on an ice surface. As reviewed by PK (1997, p. 156-157), laboratory studies e.g. by Valdez et al. (1989), Mitra et al. (1990b) and Diehl et al. (1995) indicate, however, that during the diffusional growth of ice crystals, the amounts of HNO_3 , HCl and SO_2 being incorporated into the ice are proportional to the water vapour mass converted to ice. They also show that the gas uptake by nongrowing ice crystals is favoured by the thickening of a quasi-liquid layer at the ice-air interface. In this layer, dissolution and dissociation into ions occur in a manner similar to that in bulk water. Furthermore, the experiments suggest that the amounts of adsorbed gases increase with increasing time of exposure and that the gases have difficulty in desorbing unless the ice sublimates in ice-subsaturated air.

Based on a more recent laboratory study, Diehl et al. (1998) stated that the direct uptake of gases by ice crystals is negligible compared to the gas uptake by water drops. In

spite of that, the earlier findings referred above might be interpreted as not contradicting the assumption of $c_{gs} \approx 0$, made by Chang (1984) for gases, like HNO_3 , having a high efficiency for adsorption on ice surfaces. The assumption was based on two hypotheses: firstly, under ice-supersaturation conditions, gas molecules adsorbed on the ice surface are likely to be covered by depositing water molecules. Secondly, under ice-subsaturation condition, the fraction of the ice surface sites occupied by the adsorbed molecules is too small to influence the adsorption rate significantly. In both cases, the snow scavenging of gases having high affinities for adsorption on ice may be considered as an irreversible process for which $c_{gs} \approx 0$. Further assuming an analogy with water vapour diffusion to ice particles, Chang (1984) was able to formulate an approximate expression for the rate of gas uptake by an ice particle. In the absence of more rigorous quantitative descriptions for gas scavenging by ice, the same approach is applied in the current work.

Assuming now that $c_{gs} \approx 0$ at the surface of a hydrometeor, liquid or solid, the normalized rate of irreversible gas uptake may be given as

$$J_n^{irr}(D) = 4\pi C d_g f_v, \quad (2.3)$$

where the superscript *irr* refers to irreversible, the subscript *n* refers to normalization by the ambient gas-phase concentration c_g , and C is the shape factor of the hydrometeor (PK 1997, p. 547). For liquid spheres $C = D/2$, and for ice particles, it may also be given as a function of D (e.g., Paper II). Compared to (2.2), an important feature of (2.3) is that the normalized uptake rate is now independent of c_g . It is hence analogous to the collection kernel $K_p(d, D)$ of APs, given in (2.1).

For highly soluble gases, the mass transfer from air into cloud droplets is a very rapid process. Because this process acts immediately during cloud formation (e.g., Wurzler et al. 1995), the wet deposition of such gases to the ground is not in fact controlled by in-cloud scavenging itself but rather by the precipitation efficiency of the cloud, to be discussed in the following.

2.3 Precipitation scavenging of contaminated cloud particles

Pollutants incorporated into cloud particles usually experience several cloud formation and evaporation cycles before actually being removed from the atmosphere in precipitation. Initially, the composition of cloud droplets is determined by the nucleation scavenging of APs, by the direct uptake of gases from the air and, to a less extent, by the impaction scavenging of inactivated APs; however, due to the collision and coalescence

of liquid or solid hydrometeors, the scavenged pollutants become redistributed inside the cloud water (PK 1997, p. 716). Since their main mass follows the main water mass (e.g., Respondek et al. 1995; Wurzler et al. 1995), the fraction of in-cloud scavenged pollutants actually deposited to the ground depends on the fraction of condensed cloud water that reaches the ground as precipitation (see Fig. 1). This implies that the wet removal of pollutants from the atmosphere by in-cloud scavenging is controlled by three factors: the primary in-cloud scavenging processes, the precipitation efficiency of the cloud, and the evaporation (or sublimation) of hydrometeors below cloud base.

Because the generation of precipitation in clouds mainly takes place through the collisional growth of hydrometeors, the quantity essential for the deposition to the ground of in-cloud scavenged pollutants is the collection kernel between hydrometeors of different sizes, denoted here by $K_{cl}(d, D)$. Depending on the prevailing growth mechanisms of precipitation, the relevant collection kernels are either those between liquid or solid hydrometeors, or both. On the other hand, while the definition of the collection kernel $K_p(d, D)$ in (2.1) on a number-basis is appropriate for the purpose of describing the collection of tiny APs by much larger raindrops or snowflakes, a stochastic definition of the collection kernel $K_{cl}(d, D)$ is generally needed to explain the observed growth times of hydrometeors (PK 1997, p. 622) and also the observed redistribution of chemical compounds inside the cloud water (PK 1997, p. 617). A use of the stochastic approach for assessing deposition to the ground of in-cloud scavenged species is, however, beyond the scope of the current thesis. Instead, a simpler approach will be applied, following Scott (1982) and Chang (1984).

In this approach, it is assumed that the pollutants initially scavenged by cloud-sized hydrometeors are transferred into precipitation-sized hydrometeors through collection of smaller hydrometeors by larger ones; contrary to e.g., Park et al. (1999), however, no changes in the hydrometeor sizes or water volumes are taken into account. Instead, an approximate quasi-steady-state size distribution is adopted for precipitation particles, and contaminated cloud particles are assumed to have a narrow size spectrum with the number mode at a diameter much smaller than $200 \mu\text{m}$, the conventional border between cloud and precipitation particles. In this case the collection kernel $K_{cl}(d, D)$ may be defined by analogy with (2.1), so that d and D are now the diameters of cloud-sized and precipitation-sized hydrometeors, respectively.

When different-sized hydrometeors collide with each other, they may bounce apart or break up (PK 1997, pp. 594-598). The collection efficiency $E_{cl}(d, D)$ for cloud particles therefore comprises two factors: the collision efficiency and the sticking (coalescence, retention) efficiency. As a net effect, $E_{cl}(d, D)$ typically has a maximum near the border between cloud-sized and precipitation-sized drops (Beard and Ochs 1984), albeit

turbulence and electrostatic forces may modify this behaviour. In mixed and solid-phase clouds, $E_{cl}(d, D)$ has a greater value, the larger, the more porous and the more exposed to attractive electrostatic forces the precipitation-sized ice particles are. In addition to these factors, an increasing air temperature also enhances the efficiency with which ice crystals collide with and stick to other crystals. For further discussion of $E_{cl}(d, D)$, see PK (1997, p. 581-610) and Appendix C in Paper II.

It is worth keeping in mind that, for gases like SO_2 , which have only a moderate solubility in water or efficiency for adsorption onto ice molecules, the mass transfer from air into cloud hydrometeors is a reversible process which is affected by other species present (e.g., SP 1998, p. 348-353, 379, 1027). For them, the efficiency of in-cloud scavenging as a deposition mechanism can even at best only be roughly approximated by using $K_{cl}(d, D)$.

2.4 The scavenging coefficient and related parameters

In the above, the scavenging efficiency of a single hydrometeor was considered. The overall dilution effect of a hydrometeor population is described by a precipitation scavenging coefficient. For aerosol particles and gases, respectively, it is defined as

$$\Lambda_p(d) \equiv -\frac{1}{n(d)} \frac{dn(d)}{dt} \Big|_{wet} \quad (2.4)$$

$$\Lambda_g \equiv -\frac{1}{c_g} \frac{dc_g}{dt} \Big|_{wet} \quad (2.5)$$

where $n(d)$ is the number of APs of diameter d per unit volume of air, and c_g denotes the mass concentration of the gas in air (e.g., PK 1997, p. 720, 784; SP 1998, p. 822, 1017). The notation *wet* refers to changes in time due to wet removal alone.

Definitions (2.4-2.5) allow for all kinds of wet removal processes: in-cloud and below-cloud scavenging, nucleation and impaction scavenging, irreversible and reversible gaseous scavenging. In the case of reversibly soluble gases, however, Λ_g is a function of c_g (see (2.2)) and should therefore be applied with caution.

If all the APs of size d have the same density, the number size distribution $n(d)$ in (2.4) can be replaced with the corresponding mass size distribution $n_M(d)$. For simplicity, let c denote both c_g and $n(d)$ (or $n_M(d)$) and let Λ denote both Λ_g and Λ_p . Then the rate of a concentration change in the air due to wet removal alone is equal to $-\Lambda c$. How the airborne concentrations alter as a whole also depends on the other processes involved, i.e., on the net mass inflow due to air motions of various scales and on the source terms for the

remaining processes, that is, for emissions, chemical and radioactive transformation, and dry deposition (e.g., SP 1998, p. 880).

In addition to Λ , two other parameters may also be applied in estimates of wet deposition, namely the scavenging ratio W and the scavenging factor (or scavenging efficiency) F of a pollutant. The former is defined as the ratio of the aqueous-phase concentration c_l (per unit volume of rain water) to its gas-phase concentration c (per unit volume of air). It is typically determined near the ground, and is at its best for assessing and characterizing long-term and large-scale deposition (e.g., McMahon and Denison 1979; Nordlund and Tuomenvirta 1998; Kasper-Giebl et al. 1999; Paatero et al. 2000). The latter (i.e., F) is defined as the ratio of the pollutant mass in the rain or cloud water to its mass in the air within the same unit volume of air. In other words, it gives the proportion of scavenged pollutants, and as shown later, it is particularly useful in considerations of wet deposition due to in-cloud scavenging. With the aid of the water and pollutant contents in the air and the precipitation amount, relations between Λ , W and F may be established.

2.5 The radar reflectivity factor

Besides incorporating aerosol particles and gas molecules, cloud and precipitation particles also scatter and absorb electromagnetic waves. The scattering ability of hydrometeors enables their visual observation and their remote sensing by weather satellites and radars. In addition to the dielectric properties and sizes of hydrometeors, scattering also depends on the wavelength of the incident radiation (e.g., Sauvageot 1992, p. 88). Weather radars operate in the microwave portion of the electromagnetic spectrum, using millimetre wavelengths for measurements of clouds and centimetre wavelengths for measurements of precipitation (e.g., Beard and Rauber 1990).

The quantity conventionally presented at the output of a weather radar is the equivalent radar reflectivity factor Z_e expressed in dBZ_e, that is, in decibels with respect to the value $Z_e = 1 \text{ mm}^6 \text{ m}^{-3}$. It depends on the average power \bar{P}_r of echo signals produced by a population of scatterers in a radar pulse volume, on the radar-object range r and on the attenuation of microwaves on the radar-object path. Ignoring the latter, it can be written as

$$Z_e = \frac{\bar{P}_r r^2}{C' |K|_w^2} \quad (2.6)$$

where C' is a constant that depends on the transmitted power and other properties of the radar used, and $|K|_w^2$ is the dielectric factor of liquid water, about 0.93 (Sauvageot 1992, p. 147).

By definition, Z_e is not the same as the radar reflectivity factor Z , given by

$$Z \equiv \int_{D_{min}}^{D_{max}} D^6 N(D) dD \quad (2.7)$$

where D_{min} and D_{max} are the smallest and largest diameter, respectively, of the hydrometeors (e.g., Sauvageot 1992, pp. 111). However, if the radar pulse volume is uniformly filled with a population of such hydrometeors that satisfy the conditions for the Rayleigh approximation, the two quantities are closely related:

$$Z_e = \frac{|K|^2}{|K_w|^2} Z \quad (2.8)$$

where $|K|^2$ is the average dielectric factor of the hydrometeors, equal to $|K_w|^2$ for water and about 0.208 for ice (for details, see Smith 1984).

In order to fall in the Rayleigh scattering region, raindrops have to be homogeneous spheres that are small compared with the radar wavelength. With radar using wavelengths of at least 5 cm, this condition is usually rather well satisfied (e.g., Sauvageot 1992, p. 95-96). For dry snow crystals and flakes, owing to the weak value of their dielectric factor, the application range for Rayleigh scattering is considerably broader than that for raindrops, and is practically unaffected by their deviations from sphericity (e.g., Sauvageot 1992, p. 97-102). Assuming a uniform distribution of hydrometeors in the radar pulse, one may therefore rewrite (2.8) as $Z \approx Z_e$ for rain and $Z \approx 4.5Z_e$ for dry snow. For melting ice crystals and low-density snowflakes, the relation between Z and Z_e is less well-known, while for hailstones, the Rayleigh approximation is not valid at all. On the other hand, a non-uniform scatterer distribution within the pulse volume and attenuation of radiation between the radar and the object, particularly for radar wavelengths less than about 5 cm (Sauvageot 1992, p. 107), make the dependence between Z and Z_e uncertain even for Rayleigh scatterers.

The greatest possible spatial resolution of radar data is given by the radar pulse volume, which depends on three factors: the pulse length, the width of the radar beam and the range from the radar. The smaller these factors, the smaller the pulse volume and the better this uppermost spatial resolution (e.g., Sauvageot 1992, p. 33-35). The integration time required to compute \bar{P}_r from independent samples of the echo signal power restricts the rotation speed of the antenna, and hence the highest possible temporal resolution of the data (Sauvageot 1992, p. 53-60). The maximum unambiguous range of radar measurements is limited by the pulse repetition frequency. However, since the height of the beam increases with range and the average power of received signals decrease with it (see

(2.6-2.8)), the actual coverage also depends on the sensitivity of the receiver and on the location and characteristics of the hydrometeors involved. Particularly in winter during shallow precipitation, the coverage of a single radar is likely to remain smaller than that defined by the pulse repetition frequency alone (see e.g., Joss and Waldvogel 1990). On the other hand, by using a number of elevation angles for the radar beam and a network of several radars, it is possible to obtain a three-dimensional picture of a weather system over a very large area (e.g., Collier 1999).

3 Methods and material

While the previous section mainly concentrated on various scavenging processes, in the following the more essential formulas used in Papers I-V are presented. The starting points for the theoretical study of Paper II are also discussed here. The observational data sets and methods to utilize them are then reviewed.

3.1 Basis for the $\Lambda - R$ and $\Lambda - Z$ relations

3.1.1 Irreversible below-cloud scavenging

Since the collection kernel $K_p(d, D)$ in (2.1) and the normalised gaseous uptake rate J_n^{irr} in (2.3) describe the irreversible scavenging efficiency of a single hydrometeor, the total effect of a hydrometeor population is obtained by multiplying them with a hydrometeor size distribution $N(D)$ and then integrating with respect to D . This implies that the irreversible below-cloud scavenging coefficients for APs of diameter d and gases of molecular diffusivity d_g can be written as

$$\Lambda_{pb}(d) = \int_{D_{min}}^{D_{max}} A(d, D) |V_t(D) - v_t(d)| E_p(d, D) N(D) dD \quad (3.1)$$

$$\Lambda_{gb} = \int_{D_{min}}^{D_{max}} 4\pi C d_g f_v N(D) dD \quad (3.2)$$

where the subscript b denotes below-cloud scavenging (see e.g., SP 1998, p. 1006, 1017; Chang 1984; see also Fig. 1).

The dependence of Λ_{pb} and Λ_{gb} on $N(D)$ suggests that they are closely related to the radar reflectivity factor Z ($\text{mm}^6 \text{m}^{-3}$), defined previously in (2.7), and to the precipitation

rate R (mm h^{-1}), given as

$$R = \int_{D_{min}}^{D_{max}} \frac{\pi}{6} D^3 (V_t(D) - w) N(D) dD \quad (3.3)$$

where w is the vertical component of the velocity of the ambient air. In order to analytically derive these relations, the following approximations may be made. First, the hydrometeor size distribution $N(D)$ is written as

$$N(D) = N_0 \exp(-\lambda D) \quad (3.4)$$

where N_0 and λ are referred to as the intercept and the slope, respectively. Second, the collection efficiency $E_p(d, D)$ is simplified by using

$$E_p(d, D) \approx \epsilon_p(d) \quad (3.5)$$

where the hydrometeor size-independent collection efficiency $\epsilon_p(d)$ is an estimated average of $E_p(d, D)$ at a given d (see Appendices B and C in Paper II for details). More general forms of $N(D)$ are also available (Feingold and Levin 1986; Ulbrich 1983), but unless numerical integration is used, their substitution into (3.1-3.2) is quite complicated, and they are therefore neglected here. The same is valid for formulae for the collection efficiency $E_p(d, D)$ versus D , proposed e.g. by Slinn (1977) and Murakami et al. (1985). Effects due to the fact that $E_p(d, D)$ actually has a tendency to decrease with D (Sec. 2.1.2) will be discussed later in Sec. 4.2.

Substituting now (3.4-3.5) into (2.7) and (3.1-3.3), neglecting the fall speed v_t of APs and the vertical air speed w , as compared with V_t , assuming that the other quantities involved are either constants or simple functions of D (Paper II), and then integrating from $D_{min} = 0$ to $D_{max} = \infty$ we find that for raindrops

$$\begin{aligned} \Lambda_{pb} &\propto \epsilon_p N_0 / \lambda^{3.67} \\ \Lambda_{gb} &= k_1 N_0 / \lambda^2 + k_2 N_0 / \lambda^{2.8} \\ R &\propto N_0 / \lambda^{4.67} \\ Z &\propto N_0 / \lambda^7 \end{aligned} \quad (3.6)$$

where the coefficients k_1 and k_2 depend on the gaseous molecular diffusivity d_g and the kinematic viscosity ν of the air.

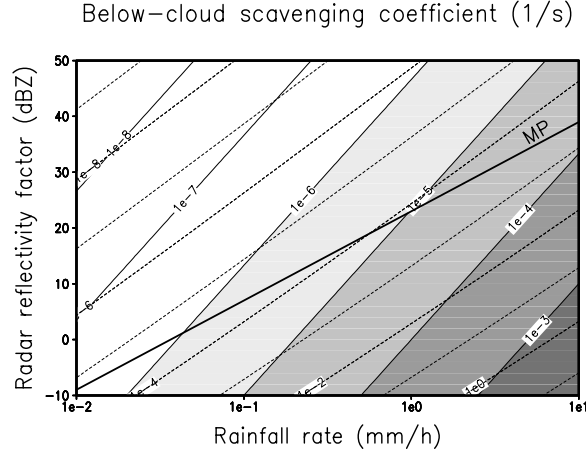


Fig. 3 Below-cloud scavenging coefficients (s^{-1}) for submicron aerosol particles (solid lines, Λ_{pb}) and highly soluble gases (dotted lines, Λ_{gb}) as a function of the rainfall rate R and the radar reflectivity factor Z . For details of the parameterizations, see Paper II. The thick solid line presents the $Z - R$ relation due to Marshall and Palmer (1948).

Relations (3.6) reveal that Λ_{pb} , Λ_{gb} , R and Z all increase with an increasing total number of hydrometeors, given by N_0/λ , and with a decreasing slope λ of the size distribution. In comparison with each other, Λ_{gb} is contributed to mainly by small hydrometeors, Λ_{pb} and R by medium-sized hydrometeors and Z by large hydrometeors. Because small hydrometeors are efficient in scavenging below-cloud pollutants but contribute weakly to Z , for a fixed R in Fig. 3, Λ_{pb} and Λ_{gb} increase with decreasing Z , i.e., with an increasing portion of small raindrops. On the other hand, assuming a fixed hydrometeor size distribution and the corresponding $Z - R$ relation, like those due to Marshall and Palmer (1948), it can be shown that Λ_{pb} and Λ_{gb} increase together with increasing Z and R (see the thick solid line in Fig. 3).

Figure 3 was constructed by eliminating both λ and N_0 from (3.6). On the other hand, elimination of λ alone results in the desired $\Lambda - R$ and $\Lambda - Z$ relations:

$$\Lambda = aR^b \quad (3.7)$$

$$\Lambda = \alpha Z^\beta \quad (3.8)$$

where the subscripts pb and gb have been omitted, and the coefficients a and α and the exponents b and β depend on the characteristics of the pollutants and precipitation. A more complete theoretical derivation of the power-law dependency (3.8) between Λ and Z , which takes into account the fact that $D_{min} > 0$ and $D_{max} < \infty$, is presented in Paper

II. The other papers included in this thesis either produce empirical estimates of the $\Lambda - R$ relationship (3.7) or utilise pre-defined relationships of the form (3.7) or (3.8).

3.1.2 In-cloud scavenging

Replacement of the precipitation particle-size distribution $N(D)$ in (3.1-3.2) by a cloud droplet size distribution produces in-cloud scavenging coefficients for APs and irreversibly soluble gases in cloud-droplet interstitial air. Nevertheless, such scavenging coefficients are not very useful, for the following reasons. Firstly, an in-cloud scavenging coefficient analogous to (3.1) does not allow for nucleation scavenging, which removes APs far more significantly than does impaction scavenging of interstitial APs (Sec. 2.1). Secondly, in-cloud scavenging of highly soluble gases, such as HNO_3 , is too rapid to limit wet deposition to the ground (Sec. 2.2). Thirdly, (3.2) is not valid for reversibly soluble gases, like SO_2 .

Paper III proposes an alternative, simple method to approximately parameterise wet removal to the ground of in-cloud scavenged pollutants. The idea is to use the scavenging factor F introduced in Sec. 2.4, together with the collection kernel $K_{cl}(d, D)$ between cloud-sized and precipitation-sized hydrometeors (Sec. 2.3). Because the integral of $K_{cl}(d, D)$ over the hydrometeors' size range gives the fractional depletion rate of the number distribution of cloud hydrometeors, in analogy with (2.4), it may be designated as a scavenging coefficient Λ_{cl} for contaminated cloud hydrometeors (Fig. 1). It is analogous to Λ_{pb} in (3.1), so that d now refers to cloud droplet diameter and ϵ_p is replaced by the average collection efficiency ϵ_{cl} between cloud and precipitation particles. Consequently, relations (3.7-3.8) with R and Z are also approximately valid for Λ_{cl} .

Now that the emphasis is laid on pollutants in cloud water, and not in rainwater, the relevant scavenging factor yields the fraction of in-cloud scavenged pollutants, and is referred to as the in-cloud scavenging factor F_{cl} (see Paper III for further discussion). If wet removal is the predominant process affecting concentrations in the air (see Sec. 2.4) and F_{cl} does not significantly change after the onset of precipitation, then the total concentration in the atmosphere is approximately given by

$$c(t) = (1 - F_{cl})c_0 + F_{cl}c_0 \exp(-\Lambda_{cl}t) \quad (3.9)$$

where c_0 is the initial concentration and t is time after the onset of precipitation at a fixed point or following the motion. The first term on the right-hand side represents the concentration in cloud-droplet interstitial air and the second term yields the pollutant mass inside cloud droplets per unit volume of air. Rearranging (3.9) produces equation (5) in

Paper III:

$$c(t)/c_0 = 1 - F_{cl}(1 - \exp(-\Lambda_{cl}t)) \quad (3.10)$$

Obviously, (3.10) reduces to a simple exponential decrease of c due to wet removal, if $F_{cl} = 1$. In that case, all the pollutants in a cloudy air layer are contained within cloud droplets or ice crystals, and one can set Λ_{cl} equal to Λ_p or Λ_g . The assumption $F_{cl} = 1$ was implicitly made by Scott (1982) and Chang (1984, 1986) when deriving in-cloud scavenging coefficients for APs and HNO_3 . Even though (3.10) is based on simple assumptions, it may offer a useful first guess for the influence of precipitation on pollutant concentrations above cloud base. In field studies, however, it is usually impossible to differentiate between F_{cl} , Λ_{cl} and Λ_{pb} or Λ_{gb} . Instead of considering collection kernels, it is more practical to use the basic definitions (2.4-2.5) for Λ and the accumulated deposition on the ground.

3.2 Wet deposition on the ground

On the basis of the definitions (2.4-2.5), the accumulated wet deposition at a fixed point on the ground during time t from the onset of precipitation can be calculated from

$$Dep_w(t) = \int_0^t \int_0^{z_t} \Lambda c \, dz' \, dt \quad (3.11)$$

where z' is the hydrometeor's path distance and z_t is the cloud top height. Usually z' is set equal to the vertical distance, assuming that the hydrometeors fall in a vertical direction through the contaminated air layer. In many cases, however, the wind transports hydrometeors considerably during their fall time. The slower their fall when compared with the wind speed, the longer and more inclined are their fall trajectories. Not only temporal and vertical, but also horizontal variations of the product Λc along the inclined trajectories hence affect Dep_w at the ground point considered. Although the wind drift of falling hydrometeors may be ignored in calculations of wet deposition with a low spatial and/or temporal resolution, as in Paper I, it is worth taking into account in small-scale wet deposition models, as shown in Papers IV and V (see also Jylhä 1996). Obviously, the use of an inclined hydrometeor's path distance z' instead of the vertical distance z implies that the fall trajectories need to be estimated and that the integrations in (3.11) have to be approximated numerically.

If wet removal is the only process affecting pollutant concentrations in the air, then

the accumulated wet deposition to the ground may alternatively written as

$$Dep_w(t) = \int_0^t \int_0^{z_b} \Lambda_{pb,gb} c_0 \exp(-\Lambda_{pb,gb} t) dz' dt + \int_0^t \int_{z_b}^{z_t} \Lambda_{cl} F_{cl} c_0 \exp(-\Lambda_{cl} t) dz' dt \quad (3.12)$$

where z_b is the cloud base height.

3.3 Observations

In order to study the $\Lambda - R$ and $\Lambda - Z$ relations (3.7) and (3.8), two data clusters were used in the present work, one gathered after the Chernobyl nuclear power plant explosion in April-May 1986 and the other during a case study near the Inkoo coal-fired power plant in December 1991. Both data clusters contain observations of the equivalent radar reflectivity Z_e by the C-band Doppler weather radar of the University of Helsinki (see Table 1 in Paper III for technical information on the radar). Additional material was also used, as reviewed in the following.

3.3.1 Data for studies related to the Chernobyl power plant

Observations made after the Chernobyl nuclear power plant explosion on 26 April 1986 and utilized in the current work may be divided into the categories described below. Paper I used data in all the categories except A4, whereas categories A3-A4 were of importance in Paper III:

- A1. Radioactivity concentrations of gamma-emitting radionuclides both in ground-level air (Bq m^{-3}) and in deposition (Bq m^{-2}) were made at four places in Southern Finland. The sampling periods varied somewhat, but the results were assumed to roughly correspond to the concentrations on 29 April.
- A2. Vertical distributions of the radionuclide concentrations (Bq m^{-3}) in the atmosphere were determined from measurements made during a research flight over Southern Finland on April 29. The measurements consisted of continuous monitoring of high-altitude gamma radiation dose rates ($\mu\text{Sv h}^{-1}$) at heights below about 3.5 km and of an air sample of particle-bound radionuclides at a height of 1.5 km.
- A3. External gamma radiation dose rates ($\mu\text{Sv h}^{-1}$) at a height of 1.5 m above the ground were measured on 29 April and 3 May 1986 by a network of radiation monitoring stations.

- A4. Equivalent radar reflectivity factors Z_e at the sites of the radiation monitoring stations (set A3) at 15 min intervals during the rainfall on 29 April were quantified on the basis of radar measurements at a constant antenna elevation angle.
- A5. Gauge-adjusted radar-derived precipitation rates R at the sites both of the concentration measurement points (set A1) and the radiation monitoring stations (set A3) at 15 min intervals on 29 April were calculated by combining the radar measurements of Z_e at a constant antenna elevation angle (set A4) with rain gauge measurements in Southern Finland.
- A6. Routine weather observations provided some information on the clouds, the phase of precipitation falling to the ground and the height of the 0°C isotherm.

In addition to the radar measurements by the University of Helsinki, data was provided by the Finnish Centre for Radiation and Nuclear Safety, the Ministry of the Interior, the Defence Forces and the Finnish Meteorological Institute. For further information, see Ilus et al. (1987), Saxén et al. (1987), Sinkko et al. (1987) and Puhakka et al. (1990), as well as Paper I, with the corrections given in the Appendix.

3.3.2 Data for studies related to the Inkoo power plant

The experiment for the collection and analysis of precipitation in the vicinity of the Inkoo power plant was carried out on 18-19 December 1991, during which period snowfall occurred in Southern Finland. Observational data gathered during the experiment and described in detail by Jylhä (1996) consist of five different sets, which are utilised in Papers IV-V:

- B1. Acidity and concentrations of sulphate (SO_4^{2-}) and some other inorganic ions at 28 sampling sites within 10 km of the power plant were analysed from 18-hourly deposition samples.
- B2. Hourly-averaged precipitation rates R at the sites of the deposition collectors were computed on the basis of continuous three-dimensional radar measurements of Z_e , also making use of reference measurements from three standard precipitation gauges.
- B3. Radiosonde measurements of the wind, temperature and humidity were carried out at a temporary sounding station in Inkoo at intervals of mainly one hour. Simultaneously, both radiosonde and Doppler radar measurements for the vertical distribution of the wind above the radar were made in Helsinki, about 60 km to the eastnortheast.

- B4. The radar antenna was manually pointed upwards at intervals of a few hours in order to measure the Doppler velocities of falling precipitation particles.
- B5. Routine measurements in the vicinity of the power plant included, among other things, collection of the monthly deposition of fly ash at four sites, measurements of hourly-averaged airborne concentrations of SO₂ at two other places, and observations of the surface wind.

These measurements were made in co-operation between the University of Helsinki, Imatran Voima Oy and the Defence Forces. For additional measurements not directly used in the present work, see Jylhä (1996).

3.4 Procedures

The experimental studies reviewed in this work all use equation (3.11) for accumulated wet deposition Dep_w and either the $\Lambda - R$ relationship (3.7) or the $\Lambda - Z$ relationship (3.8). Consequently, some estimates of the spatial and temporal distribution of Λ and the airborne pollutant concentration c are needed in all of them:

- A typical vertical profile of the radionuclide concentrations c is estimated in Paper I from the aircraft measurements (set A2). Horizontal variations in c and the wind drift of raindrops are ignored, and little attention is paid to changes of c in time. In Paper III, this simplified distribution of c is implicitly adopted, too. In Papers IV-V, on the other hand, the temporal and spatial distribution of c is calculated from a Gaussian plume equation, using radiosonde observations (set B3) as the meteorological input data. The wind drift of contaminated hydrometeors is taken into account with the aid of Doppler radar measurements of their fall speeds (set B4).
- Scavenging coefficients Λ are calculated from gauge-adjusted radar precipitation rates R on the ground (sets A5 and B2; Papers I and IV-V) or from equivalent radar reflectivity factors Z_e along the inclined radar beam (set A4; Paper III). Because it is not possible to distinguish between in-cloud and below-cloud scavenging, the resultant values are assumed to approximate the vertical averages of Λ either over the whole polluted air layer (Papers I, III and V) or separately above and below the 0°C isotherm (Paper IV).
- The empirical $\Lambda - R$ relationships (3.7) are determined by searching out those values of a and b (Paper I) or a alone, with a fixed b (Paper V) which produce the best agreement between observed and modelled wet depositions. Data from

four stations (set A1), together with assessed degrees of uncertainty in the factors involved, enable limits of error to be estimated in Paper I. In Papers III and IV, predefined $\Lambda - R$ or $\Lambda - Z$ dependencies are used to assess Λ .

4 Results and discussion

4.1 The $\Lambda - R$ relationship

4.1.1 Results of studies related to the Chernobyl power plant

After the accident at the Chernobyl nuclear power plant in the Ukraine on 26 April 1986, the first observations in Finland of temporary increases in radioactivity near the ground, made on 27 April, were related to the passage of a polluted air mass containing gases and particles from the initial explosion of the nuclear reactor (Savolainen et al., 1986; Sinkko et al. 1987; Arvela et al. 1990; Puhakka et al. 1990). The second major peak of radionuclide concentrations in ground level air was observed on 29 April (Sinkko et al. 1987), when a widespread rainfall area affected Finland (Savolainen et al., 1986; Puhakka et al. 1990). Aircraft measurements on that day indicated that radioactive substances mainly arrived over Finland at heights between 1-3 km, the maximum being at a height of about 1.5 km (Sinkko et al. 1987). In terms of their activity concentrations, the most abundant gamma-emitting radionuclides aloft, in ground-level air and in deposition were isotopes of iodine (I), tellurium (Te), cesium (Cs), ruthenium (Ru) and barium (Ba). The increases in radioactivity near the ground typically occurred almost simultaneously with the onset of rainfall (Puhakka et al. 1990). In Helsinki, for example, the activity concentrations in ground-level air increased by an order of 10-100 reaching values of 0.5 Bq m^{-3} for ^{137}Cs and 5 Bq m^{-3} for ^{131}I , although the amount of rain was very small (Puhakka et al. 1988). At Uusikaupunki, where the highest external gamma radiation dose rates in ground-level air were observed, the rise from about 0.2 to $4.0 \mu\text{Sv h}^{-1}$ likewise took place during or immediately after the period of the most intensive precipitation.

The empirical relationships between the ground-level rainfall rate R and the vertically-averaged scavenging coefficient Λ for the gamma-emitting radionuclides involved, estimated in Paper I from the radioactivity and gauge-adjusted radar measurements in Southern Finland, are presented in Table 1 with the assessed limits of error. The relationships describe scavenging by hydrometeors mostly in the liquid phase, and comprise the total effect of in-cloud and below-cloud wet removal within the whole polluted layer from the ground level up to about 3 km.

Table 1 Empirical relations $\Lambda = aR^b$ between the scavenging coefficient Λ (s^{-1}) of different radionuclides, originating at Chernobyl, and the rainfall rate R ($mm\ h^{-1}$) in Southern Finland on 29 April 1986. Activity concentrations ($Bq\ m^{-3}$) of the nuclides at a height of 1.5 km are also shown (based on Paper I and Sinkko et al. 1987).

Nuclide	$\Lambda = aR^b$		$c(1.5\ km)$
	a (s^{-1})	b	
^{103}Ru	$(4\pm 3)\cdot 10^{-4}$	0.72 ± 0.09	28.5
^{106}Ru	$(2\pm 2)\cdot 10^{-4}$	1.2 ± 0.2	27.0
^{129m}Te	$(1.3\pm 1.2)\cdot 10^{-4}$	0.4 ± 0.2	52.0
^{132}Te	$(1.8\pm 1.2)\cdot 10^{-4}$	0.71 ± 0.11	420.0
$^{131}\text{I(p)}$	$(7\pm 5)\cdot 10^{-5}$	0.69 ± 0.12	690.0
$^{133}\text{I(p)}$	$(1.6\pm 1.3)\cdot 10^{-5}$	0.5 ± 0.2	77.0
^{134}Cs	$(2.8\pm 0.6)\cdot 10^{-5}$	0.51 ± 0.07	97.0
^{136}Cs	$(2.4\pm 0.5)\cdot 10^{-5}$	0.43 ± 0.08	35.0
^{137}Cs	$(3.4\pm 0.9)\cdot 10^{-5}$	0.59 ± 0.08	167.0
^{140}Ba	$(3\pm 2)\cdot 10^{-5}$	0.3 ± 0.5	65.0

On the basis of the average values of a and b in Table 1, weighted by the high-altitude nuclide concentrations $c(1.5\ km)$, a relation

$$\Lambda = 1 \cdot 10^{-4} s^{-1} R^{0.64} \quad (4.1)$$

was proposed in Paper I to have been typical for the nuclides involved. Another rather similar relation,

$$\Lambda = (8 \pm 2) \cdot 10^{-5} s^{-1} R^{0.65\pm 0.02} \quad (4.2)$$

is suggested by the solid curve with error bars in Fig. 4. In constructing that curve, which is nearly a straight line, the values of a and b in Table 1, with the limits of error, were used to evaluate Λ and its relative error separately for each type of radionuclide. A weighted average of Λ was then calculated as a function of R , applying this time weights that depended both on the concentrations aloft and on the relative errors. A logarithmic plot of Λ versus R in Fig. 4 finally enabled the average relation (4.2) to be obtained.

For comparison, Fig. 4 also presents theoretical $\Lambda - R$ relations for SO_4^{2-} , NO_3^- and HNO_3 in rain due to Scott (1982) and Chang (1984, 1986), as well as an empirical layer-averaged relation for SO_4^{2-} due to Okita et al. (1996). Two features are readily seen: the curve for the Chernobyl-derived radionuclides has almost the same slope as the other curves, and it lies between those for in-cloud and below-cloud scavenging. The former is

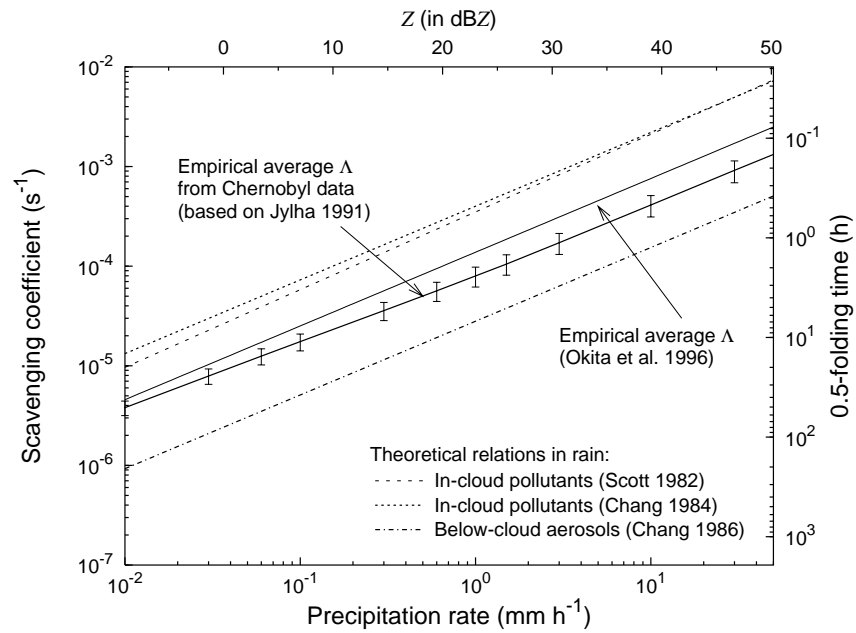


Fig. 4 Empirical average scavenging coefficient Λ for particle-bound radionuclides from Chernobyl as a function of precipitation rate R in Southern Finland on 29 April 1986, with limits of error. Also shown are other $\Lambda - R$ relations from various authors. The secondary vertical and horizontal axes indicate the 0.5-folding time and the radar reflectivity factor, respectively, assuming the $Z - R$ relation due to Marshall and Palmer (1948).

due to the relatively small variation in the exponent b of the $\Lambda - R$ relation, and the latter may be attributed to the fact that both in-cloud and below-cloud removal probably contributed to the Chernobyl-derived fallout in Southern Finland. The good correspondence between the curves for the radionuclides and for the inorganic ions may be explained by the findings of studies of the radionuclide size distributions (e.g., Jost et al. 1986; Kauppinen et al. 1986). Since the size distributions of Chernobyl-derived ^{132}Te , ^{103}Ru and ^{137}Cs resembled those of sulphate, nitrate and ammonium ions, it is probable that the nuclides were attached to aerosol particles at quite an early stage and that their removal mechanisms were quite similar to those for the inorganic ions. Owing to this similarity, the results obtained in Paper I and reviewed here may also be relevant for the wet deposition of SO_4^{2-} and NO_3^- .

The relationships in Table 1 are based on only a few cases with light rain, while in some other parts of Southern Finland even thunderstorms with hail occurred (Puhakka et al. 1990). In spite of that, they appeared on average to be fairly suitable for estimating external gamma radiation dose rates at a height of 1.5 m above the ground within the whole study area. This is indicated by Fig. 5, which shows the assessed dose rates on the next day of available radiation measurements, 3 May, as a function of the corresponding observations (set A3). The percentage of estimates that agree with observations to within

a factor of two is 76%, and there is a significant positive correlation between them, with a logarithmic correlation coefficient of 0.66 (p -value = 0.001).

Possible reasons for the scatter in Fig. 5 include temporal and spatial variations in the distributions of hydrometeors and particle-bound radionuclides, uneven dry deposition patterns, contribution of gaseous nuclides, occurrence of so-called hot particles, possible extra wet deposition between 29 April and 3 May, variations in natural background radiation in the range of 0.05-0.18 $\mu\text{Sv h}^{-1}$ (Arvela et al. 1990) and, perhaps, measurement errors (see Paper I for details). Taking the large number of potential error sources into account, the observations and predictions agree surprisingly well with each other. This confirms the notion of the importance of precipitation in depositing radioactive materials onto the ground, and also supports the empirical $\Lambda - R$ relationships presented in Table 1.

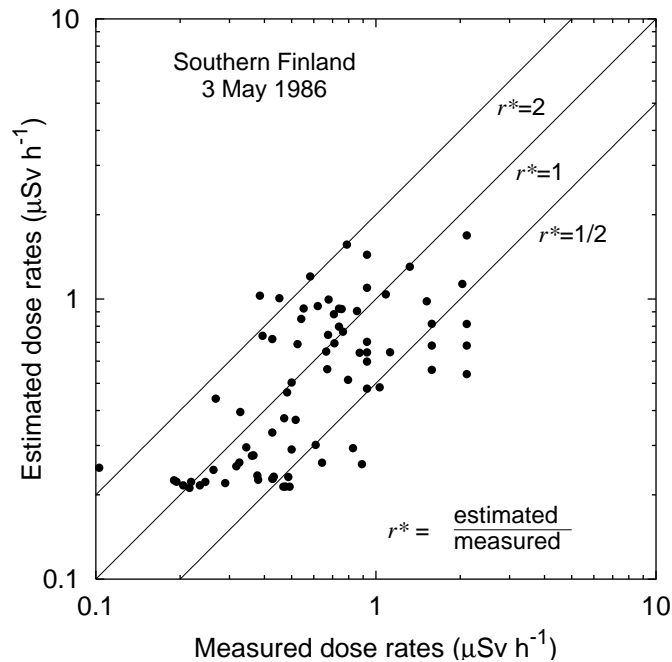


Fig. 5 Estimated and observed gamma radiation dose rates in Southern Finland on 3 May, and the ratio r^* between them (based on Jylhä 1990).

It may finally be noted that the upper horizontal axis in Fig. 4 was constructed to represent the logarithmic radar reflectivity factor dBZ assuming the $Z - R$ relation due to Marshall and Palmer (1948). The figure hence indirectly reveals power law dependences of the form (3.8) between Λ and Z , to be discussed more closely in Sec. 4.2. The secondary vertical axis in Fig. 4 gives in turn the 0.5-folding time $\tau_{0.5} = \ln 2 / \Lambda$, that is, the time period required for precipitation scavenging to reduce the concentrations in the air by half in the case of no compensation by a net inflow or other supplies of pollutants.

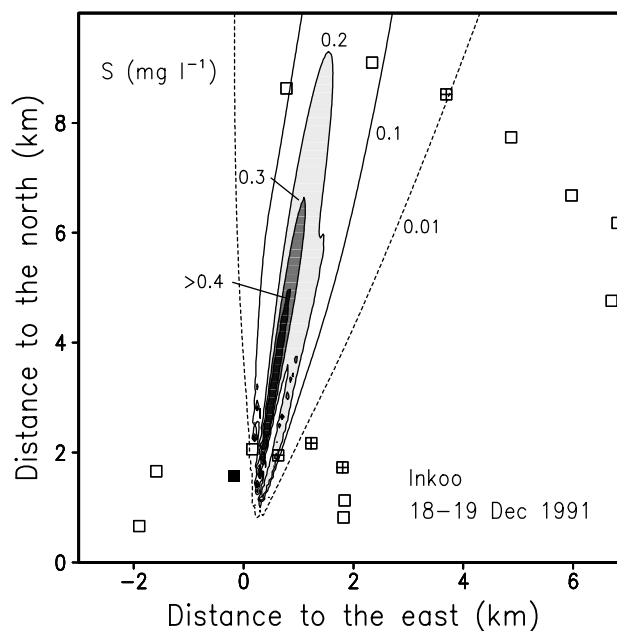


Fig. 6 *Estimated horizontal distribution of sulphur concentration (mg l^{-1}) in wet deposition due to emissions from the Inkoo power plant at point (0,0) on 18-19 Dec 1991. Solid, open and crossed squares show samples with an acidity of 4.0, 4.1 and 4.2 pH-units, respectively (based on Paper V).*

4.1.2 Results of studies related to the Inkoo power plant

An appraisal of the $\Lambda - R$ relationship for SO_2 and primary SO_4^{2-} in snow within the first 10 km of the source is presented in Paper V. The original goal of the wintertime case study considered in that paper and in the accompanying preliminary paper IV was to analyse wet deposition near a 250 MW coal-fired power plant unit at Inkoo on the south coast of Finland, and to find out whether it was possible to identify any influence of the power plant emissions on local wet deposition. By chance, the experiment was carried out during an episode of strong long-range transport of pollutants from Central Europe. Moreover, the power plant plume missed most of the measurement points, a fact that emerged from both the preliminary model calculations in Paper IV and the more final results of Paper V, the latter being redrawn in Fig. 6. These two facts diminished the possibility of recognising the effects of the source on wet deposition. Emissions from the power plant did increase the concentrations of SO_2 in ground-level air by a factor of 2 to 10 at a downwind distance of about 2 km (Fig. 2 in Paper V), but no reliable signs of the influence of the power station on the sulphate deposition could be identified: concentrations of non-sea-salt sulphate in the deposition samples varied around a mean value of 1.8 mg(S) l^{-1} without any discernible increase downwind of the power station (Fig. 2 in Paper IV and Fig. 5 in Paper V).

On the basis of the preliminary model estimates presented in Paper IV, it should have been possible to detect the additional sulphur load due to the power station emissions in one or two deposition samples. Because the observations did not, however, reveal any reliable sign of this load, it is probable that the predefined $\Lambda - R$ relationships, at least that for primary SO_4^{2-} at temperatures below zero (Chang 1986), overestimated wet deposition of sulphur species within the first 10 km from the source. Instead, the relationship

$$\Lambda \leq 10^{-6} \text{ s}^{-1} R^{0.7} \quad (4.3)$$

was found to produce wet deposition estimates that were not in contradiction with the observations. Assuming this relationship, the modelled concentrations of primary sulphur remained below 0.2 mg(S) l^{-1} at the collector sites, and ranged at most between about $0.4\text{-}1.0 \text{ mg(S) l}^{-1}$ in a narrow area at downwind distances of about 1-5 km (Fig. 6). This means that at the collector sites the modelled contribution of the local source did not exceed the variation in the dominating background level, about 0.2 mg(S) l^{-1} . On the other hand, as the highest values predicted by the model were approximately one half of the background concentrations measured outside the plume sector, one may speculate that if the sampling network had been denser than that used, it might have been possible to discern some plume-related sulphur deposition.

Equation (4.3) provides an uppermost limit for the vertically-averaged scavenging coefficient of sulphur within the first 10 km downwind of the source as a function of ground-level precipitation rate. Nevertheless, because it was assessed indirectly by making some kind of adjustment of the model results with the chemical analysis outcomes, it is highly sensitive to uncertainties in the shape of the plume, in the emissions, wind profiles, precipitation intensities and fall speeds of snow particles. The influence of the fall speed is readily seen in Fig. 7: except in the immediate vicinity of the chimney, precipitation particles having slow fall speeds, and hence inclined fall trajectories, have a chance of collecting more pollutants during their fall through the plume than those falling in a vertical direction. Additionally, pollutants attached to such hydrometeors deposit on the ground at a greater range from the source than those incorporated into more vertically-falling hydrometeors. Since the wind drift of precipitation particles so modifies small-scale wet deposition patterns, it had to be taken into account here, and is in general worthy of attention when precipitation scavenging is studied at a high spatial and temporal resolution.

The wet deposition pattern in Fig. 6, when combined with information on total amounts of precipitation and emissions, suggests that the percentage of emitted sulphur being scavenged within the study area was equal to or less than about 0.7%. Although being near their lower limit, this estimate agrees with previous experimental studies around

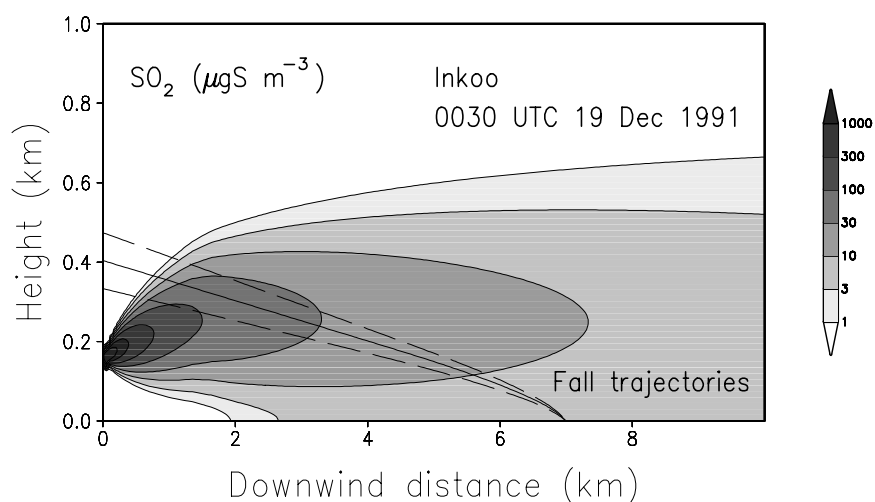


Fig. 7 *Estimated vertical distribution of SO_2 concentration ($\mu\text{gS m}^{-3}$) along the plume axis at 0030 UTC on 19 Dec 1991 due to releases from the Inkoo power plant. The fall trajectories of snowflakes having a fall speed of $0.7 \pm 0.14 \text{ m s}^{-1}$ and an identical landing point are also shown (based on Paper V).*

point sources, according to which the percentage typically ranges from less than 1% to about 6-8% (see Paper V for a review). This agreement may be taken as support for the semiempirical $\Lambda - R$ relationship (4.3). Consequently, it seems likely that snowfall at temperatures close to 0°C was rather inefficient in scavenging freshly-emitted S. The observed variations in sulphate concentrations in the precipitation were rather caused by variations in the background level, and these at least partly resulted from unequal sampling periods (Jylhä 1996). Nevertheless, a suspicion lingers that the acidifying and/or acid-neutralizing releases from the power plant did produce the observed features in the horizontal pattern of acidity.

The snowfall samples collected during the experiment were rather acid, with a mean pH of 4.1 (see the notations in Fig. 6, Fig. 2 in Paper IV or Fig. 5 in Paper V). As the observed deviations from the mean were concentrated in one sector not far from the modelled area of deposited plume pollutants, efforts were made in Paper V to explain them with the aid of the power plant emissions. However, because of an analysis resolution of no better than 0.1 pH-units, a fairly sparse deposition sampling network and uncertainties attached to the model estimates, the role of the local emissions could neither be confirmed nor totally rejected. Although plume-related sulphur and hydrochloride (HCl), in particular, added to the acidity, while alkaline fly ash particles acted to neutralise it, their modelled concentrations in deposition at the sites of the collectors were too low to explain the observed shifts in pH from 4.1 to 4.0 or to 4.2. The deposition sector of acidic emissions should have been more westerly and that for the fly ash more easterly than pro-

posed by Fig. 6, in order that they could possibly account for the observed deviations in pH. Supposing that the wind direction observations were unbiased, this means that acidic gases should have risen at least 200-300 m higher than expected, but in that case they would have been too elevated to reach the collector having a pH of 4.1 (see Jylhä 1996). On the other hand, because the majority of the fly ash mass was presumably concentrated into particle sizes much less than 20 μm (see Kauppinen and Pakkanen 1990), no significant sinking of ash particles due to gravity could be expected. The effects of the local emissions on the acidity of precipitation therefore remain unproven.

4.2 The $\Lambda - Z$ relationship

4.2.1 Theoretical dependencies

In Papers I and IV-V, gauge-adjusted radar measurements of the precipitation rate R were used to estimate Λ . Another possibility, proposed in Papers II and III, is to evaluate Λ with the aid of the radar reflectivity factor Z . There are not, however, any universal $\Lambda - Z$ relations for below-cloud and in-cloud pollutants; they depend on the properties of the precipitation and pollutants. In Paper II, two types of precipitation particles are considered, namely liquid drops in stratiform rain and dry ice-crystal aggregates, and in both cases their size spectrum is assumed to be exponential (Eq. (3.4)). The emphasis is laid on below-cloud aerosol particles in the size range of 0.3-0.9 μm , on below-cloud gases with a high solubility in water and affinity for adsorbing on ice, and on cloud particles much smaller than precipitation particles. The size range was selected on the basis of the measured activity size-distributions of particle-bound radionuclides in Finland after the accident at the Chernobyl nuclear power station (Kauppinen et al. 1986). A substantial part of other anthropogenic aerosol particles is also found concentrated in that size range (Seinfeld and Pandis 1998, p. 431).

The resulting theoretical dependencies between Λ and Z are not exactly of a power-law form of (3.8), as indicated by the slightly bending dotted curves on the logarithmic plots of Figs. 8-9, but they can be approximated as such. As an example, for pollutants in cloud droplets during stratiform rain, it was found in Paper II that

$$\begin{aligned} \Lambda &\approx 1.4 \cdot 10^{-5} \text{ s}^{-1} Z^{0.59}, & 10^{-1} \leq Z < 10^1 \text{ mm}^6 \text{ m}^{-3} \\ \Lambda &\approx 1.5 \cdot 10^{-5} \text{ s}^{-1} Z^{0.53}, & 10^1 \leq Z < 10^5 \text{ mm}^6 \text{ m}^{-3} \end{aligned} \quad (4.4)$$

According to these formulae, as well as the corresponding $\Lambda - Z$ relations for below-cloud submicron APs and highly soluble gases (Table 2 in Paper II), the exponent β in the

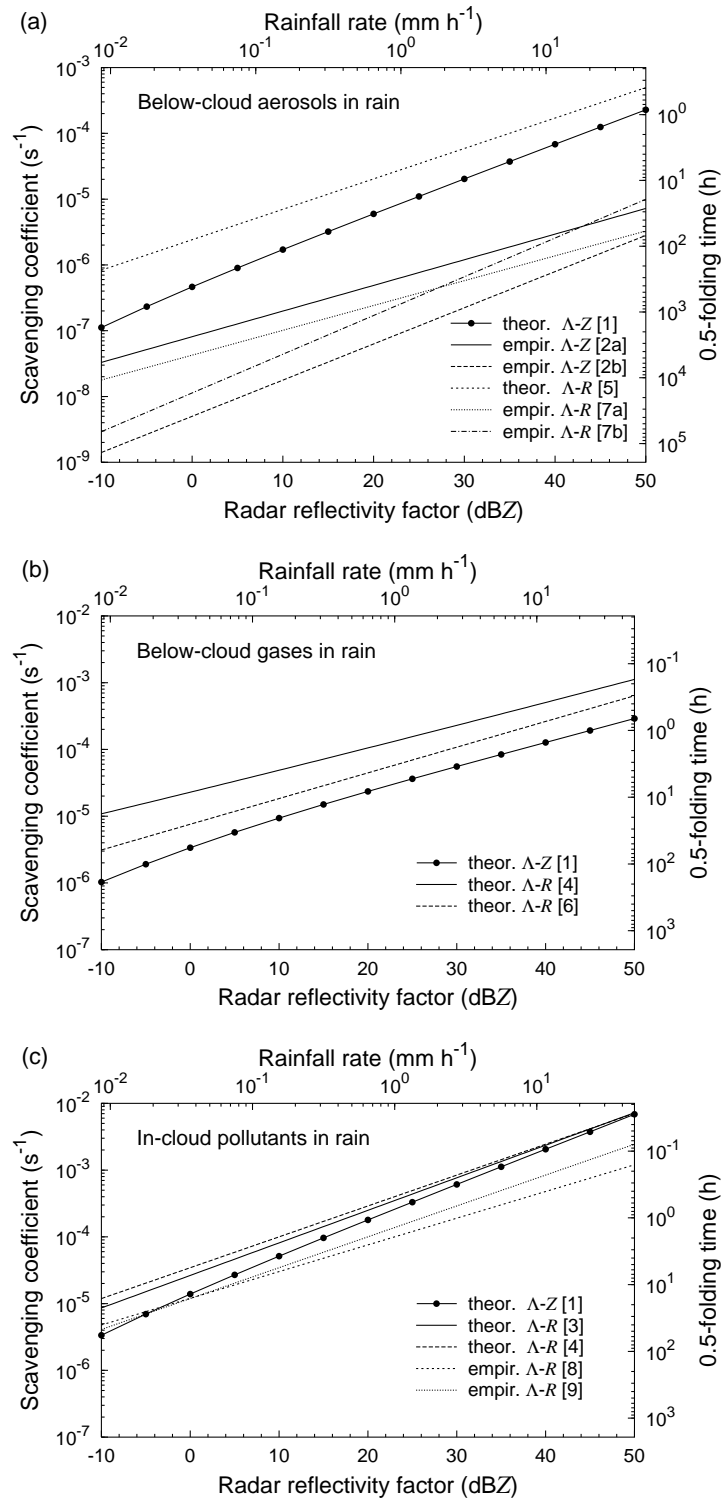


Fig. 8 Theoretical and empirical dependencies between the scavenging coefficient Λ in rain and the radar reflectivity factor Z (and also the precipitation rate R) for (a) below-cloud submicron aerosol particles in rain, (b) below-cloud highly soluble gases in rain and (c) pollutants in contaminated cloud droplets. For construction of the upper horizontal axes, the $Z - R$ relation due to Marshall and Palmer (1948) has been assumed. The right-hand vertical axes indicate the 0.5-folding time. Note the differing vertical scale in (a). For additional information, see Table 2 and Paper II.

relation $\Lambda \approx \alpha Z^\beta$ lies in the case of rain between about 0.4 and 0.6. As shown by Fig. 8, this implies that an increase in Z by a factor of 10 approximately results in an increase in Λ by a factor of 2.5-4. Furthermore, the 0.5-folding time, defined previously in Sec. 4.1.1, decreases by the same factor.

In snowfall, the dependence of Λ on Z is more uncertain, because of the large variety of types and shapes of solid hydrometeors. For dry ice crystal aggregates, Paper II proposes that the dependence is weaker than for raindrops: the exponent β is about 0.1-0.2 for below-cloud gases and 0.2-0.4 for below-cloud APs and in-cloud pollutants. Accordingly, the curves for the snow scavenging coefficients in Fig. 9 slope more gently with Z than those for the rain scavenging coefficients in Fig. 8. On the other hand, because in snow the equivalent radar reflectivity factor Z_e is typically about 7 dBZ smaller than the radar reflectivity factor Z (Sec. 2.5), it can be shown that at the moderate values of 0-35 dBZ_e, the scavenging coefficient for contaminated cloud hydrometeors differs by only a factor of 2 at most between snow and rain (see Fig. 2 in Paper III).

By adopting the $Z - R$ relations due to Marshall and Palmer (1948) and Sekhon and Srivastava (1970), the theoretical and empirical $\Lambda - R$ relations from various authors were converted in Paper II into $\Lambda - Z$ relations. For the sake of comparison, these results, as well as the semiempirical $\Lambda - Z$ relations of Seliga et al. (1989), are included in Figs. 8-9 (for additional information, see Table 2). The figures suggest that more uncertainty is attached to the below-cloud scavenging coefficient Λ_{pb} than to the scavenging coefficient

Table 2 *References in Figs. 8-9.*

Label	Authors	Remarks
$\Lambda - Z$ relations		
1	Jylhä (1999a)	Theoretical (this work)
2a	Seliga et al. (1989)	Semiempirical for $d=0.4 \mu\text{m}$
2b	Seliga et al. (1989)	Semiempirical for $d=1.0 \mu\text{m}$
$\Lambda - R$ relations		
3	Scott (1982)	Theoretical
4	Chang (1984)	Theoretical
5	Chang (1986)	Theoretical
6	Asman (1995)	Theoretical, convective rain
7a	Sparmacher et al. (1993)	Empirical for $d=0.46 \mu\text{m}$
7a	Sparmacher et al. (1993)	Empirical for $d=0.98 \mu\text{m}$
7c	Sparmacher et al. (1993)	Empirical for $d=1.66 \mu\text{m}$
8	Jylhä (1991)	Empirical, layer-averaged
9	Okita et al. (1996)	Empirical, layer-averaged
10	Jylhä (2000)	Semiempirical, upper limit

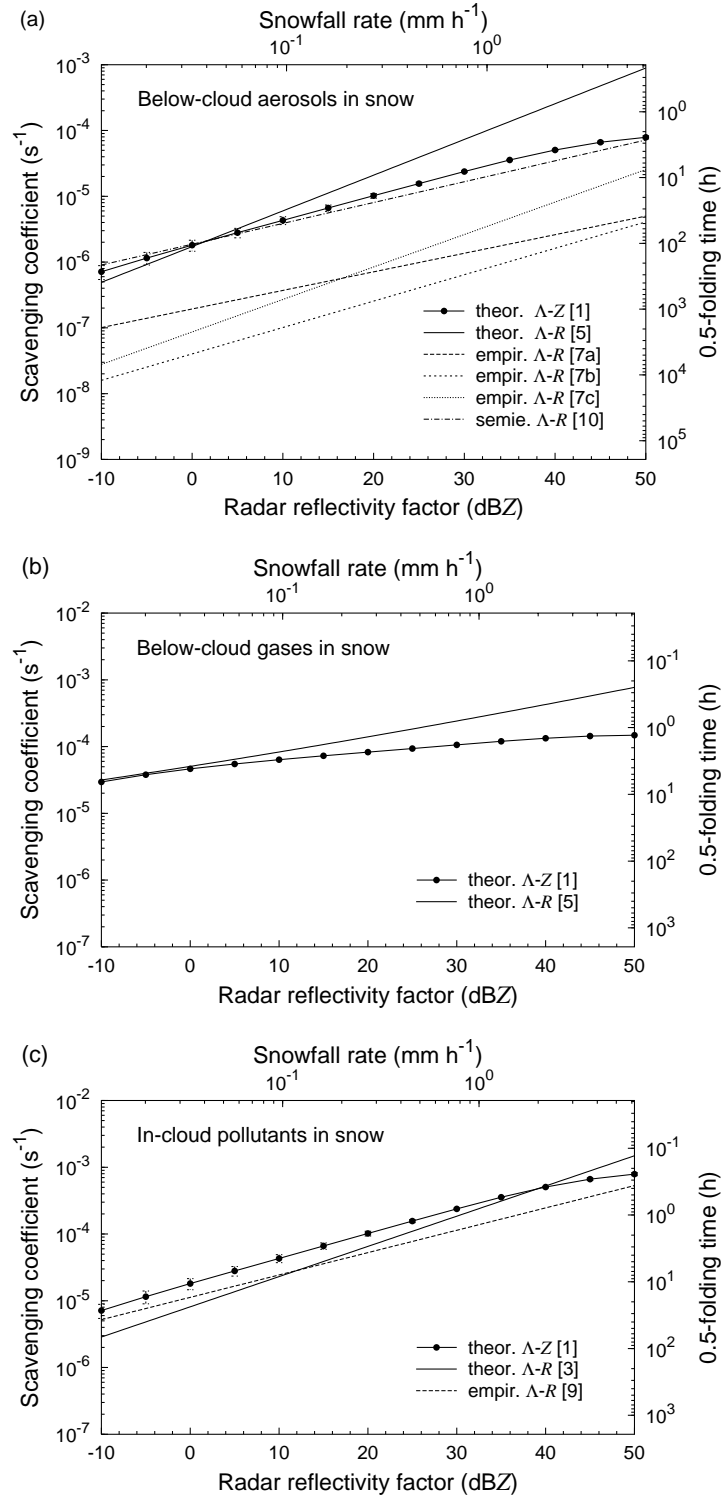


Fig. 9 As Fig. 8, but for snow. For construction of the upper horizontal axes, the $Z - R$ relation due to Sekhon and Srivastava (1970) has been assumed. The error bars refer to alternative dependencies of the fall speed V_t on the ice particle size D . For additional information, see Table 2 and Paper II.

Λ_{cl} of contaminated cloud droplets. This probably ensues from the dependence of the collection efficiency $E(d, D)$ on the sizes of colliding bodies. While the collection efficiency by precipitation particles is rather well known for cloud hydrometeors, even its order of magnitude is uncertain for submicron APs (see Paper II). Since the tendency of $E_p(d, D)$ to decrease with D is ignored (see Eq. 3.5), the exponent β of theoretical $\Lambda_{pb} - Z$ relations may be slightly overestimated, as can be inferred from (3.6).

One reason for the deviations between the theoretical curves in Figs. 8-9 is the fact that Scott (1982) and Chang (1984, 1986) assumed untruncated hydrometeor size distributions and hence presumably got overestimated values of Λ in light rain and in heavy snow. All the theoretical curves in Figs. 8-9, whether or not based on the truncated integration limits in (3.1-3.2), are probably at their most accurate at intermediate values of Z , maybe between about 10 and 40 dBZ. This is due to the fact that they all rest upon simplified hydrometeor size distributions which are based on a limited range of precipitation rates (Marshall and Palmer 1948; Sekhon and Srivastava 1970). For convective rain and wet snow, on the other hand, the curves are even at best only very approximate, while for hail they are presumably not applicable at all.

For below-cloud gases, a difficulty arises from the fact that Λ_{gb} is weighted in favour of small and Z in favour of large hydrometeors (Sec 3.1.1). A few large hydrometeors may produce a large value for Z , but will scavenge gases relatively ineffectually. In snowfall, Λ_g appears to be nearly independent of Z (Fig. 9). Thus in wet deposition estimates of below-cloud gases the duration of snowfall might be a more relevant quantity to be considered than the exact value of Z .

According to Fig. 8, at all values of Z rain scavenges pollutant-containing cloud droplets far more efficiently than below-cloud pollutants. Hence if pollutants are distributed uniformly below and above cloud base, wet deposition due to in-cloud scavenging dominates. This is also valid for snowfall, excepting perhaps light snow in the case of gaseous pollutants. On the other hand, if the height of the polluted air layer with respect to the 0°C isotherm and the radar beam is unknown, one can recommend the use of $\Lambda - Z$ relationships for rain even at heights above the melting layer, as deliberated more closely in Paper III. Among the theoretical $\Lambda - Z$ relations in Figs. 8-9 and Paper II, the most essential are therefore those for pollutant-containing cloud droplets during stratiform rain, i.e. equations (4.4).

In the case of pollutants with characteristics deviating from those assumed here, only simple modifications are needed in order to make use of the theoretical $\Lambda - Z$ relations in Figs. 8-9. Because Λ_{gb} is directly proportional to the gaseous diffusivity d_g of below-cloud highly soluble gases, while Λ_{pb} and Λ_{cl} depend on the average collection efficiencies $\epsilon_p(d)$ and $\epsilon_{cl}(d)$, respectively, (see (8) in Paper II), they only have to be multiplied by the

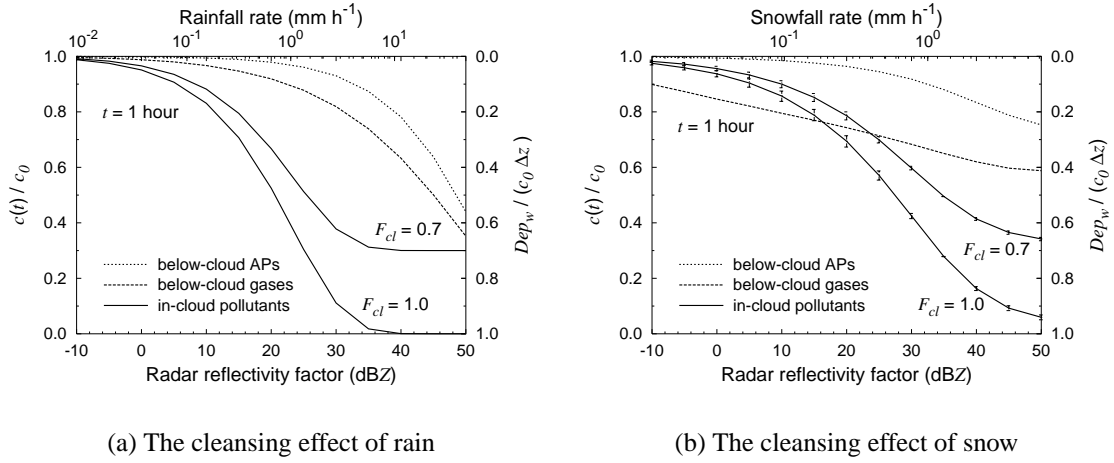


Fig. 10 Theoretical dependence of the ratio between prevailing and initial concentrations in the atmosphere after one hour of uniform precipitation as a function of the radar reflectivity factor Z for below-cloud highly soluble gases and submicron aerosol particles, and for pollutants in contaminated cloud droplets with an in-cloud scavenging efficiency F_{cl} of 0.7 or 1.0. No compensation of the cleansing effect is assumed. Also shown is the corresponding dimensionless accumulated wet deposition. For the error bars in (b), see Fig. 9 (based on Paper III).

ratio between the new and original values of d_g , $\epsilon_{pb}(d)$ or $\epsilon_{cl}(d)$.

Finally, it can be shown using the $\Lambda - Z$ dependencies derived in Paper II that, although the cleansing effect of precipitation is minor during periods of small and moderate values of Z , significant amounts of pollutants may be deposited onto the ground, provided that the concentrations c in the atmosphere are high enough (Fig. 10). If not all the pollutants residing above cloud base are attached to cloud droplets ($F_{cl} < 1$), the accumulated wet deposition is reduced accordingly (Fig. 10). On the other hand, if the scavenging of pollutants is partly compensated by a net inflow or other supply of pollutants, then larger amounts of pollutants will be deposited onto the ground than presented in Fig. 10. In fact, if the compensation is more or less complete, so that c remains practically constant in time, the accumulated wet deposition is almost linearly proportional to the time integral of Λ , and therefore strongly depends on Z . As shown below, this approximation may be adopted to make a first estimate of wet deposition; such an estimate might be required in a potential emergency after an accidental release of hazardous materials into the atmosphere.

4.2.2 An example related to Chernobyl

The observed gamma radiation dose rates in ground-level air in Southern Finland on 3 May 1986, following the Chernobyl accident, presented previously in Fig. 5 as a function

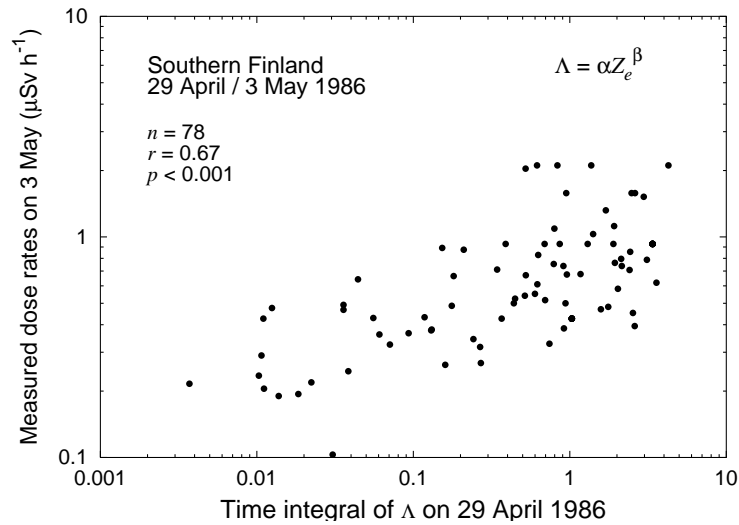


Fig. 11 Measured gamma radiation dose rates in ground-level air in Southern Finland on 3 May 1986, following the Chernobyl accident, as a function of the time integral of the radar-derived in-cloud scavenging coefficient Λ on 29 April 1986. Sample size n , logarithmic correlation coefficient r and p -value are also shown (based on Paper III).

of the estimated dose rates, are now shown in Fig. 11 as a function of the time integrals of a single factor, the radar-derived scavenging coefficient Λ on 29 April. This time, the dose rates are assumed to roughly stand for the actual wet deposition on 29 April due to the rain on that day. The positive relation between them and the time integrals, with a logarithmic correlation coefficient of 0.67 (p -value < 0.001), is about the same as found in Fig. 5 for the observed and estimated dose rates. The time integrals of Λ , which were calculated from the original radar measurements of Z_e using (2.8) and (4.4), seem therefore to be quite good in approximating the accumulated wet deposition (3.11) in relative terms. This supports the $\Lambda - Z$ relationship (4.4) and also indicates that even measurements of radar reflectivity alone, without any information about the airborne concentrations aloft, may be very useful in pin-pointing the areas presumably contaminated by wet deposition.

In Fig. 11, an increase of the time integral of Λ by a factor of 10 corresponded, on average, to an increase in the dose rates of 75 per cent. On the other hand, one may speculate that if the source of the pollutants had been nearer the precipitating weather system, so that larger amounts of airborne pollutants had been exposed to the wet removal processes, the measured dose rates might have been even more strongly correlated with the time integrals of Λ than in Fig. 11. Since in this case the measured magnitudes of radioactivity were near the minimum detectable value (Puhakka et al. 1990), horizontal variations of natural background radiation, dry deposition and radioactive decay between 29 April and 3 May most likely lowered the correspondence. Additional explanations for the scatter in Fig. 11 are the uneven temporal and spatial distribution of the pollutants in

the atmosphere and the variation of Z_e with height (see also discussion regarding Fig. 5 in Sec. 4.1.1).

In Paper III, only data from a single weather radar and one elevation angle were used, so that the height of the radar measurements increased with range; the three-dimensional distribution of Z_e is unknown. Although it was not possible to identify any apparent effects of the height of the radar beam axis on the scatter in Fig. 11, the Z_e -derived values of Λ underestimated wet deposition at long ranges from the radar. This was verified by recalculating the time integral of Λ , using now the empirical relationships (4.1) between Λ and the gauge-adjusted radar precipitation rate R . Most likely, however, the tendency of underestimating with range had little to do with the relationships used between Λ , Z and R , but ensued from beam overshooting of precipitation (see Sec. 2.5). The mean ratio between the values of the time integrals of Λ due to the $\Lambda - Z_e$ method to those due to the $\Lambda - R$ method was close to unity, which indicates that (4.4) was rather good in approximating wet removal of the radioactive materials involved in this study. This finding, combined with the fact that the radar reflectivity factor can be measured in real-time over wide areas, supports its use to provide a first estimate of precipitation scavenging.

4.3 The use of weather radar in wet deposition estimates

4.3.1 General aspects

The main questions in the case of wet deposition are the following: What is the strength and areal distribution of the deposition? How large a portion of pollutants remains in the atmosphere in spite of the precipitation and is then transported to other areas with the wind? In order to reply to these questions, it is necessary to appraise three components: the dispersion of the air pollutants, the occurrence and strength of precipitation on the track of the air pollutants, and the efficiency with which the precipitation scavenges them. Assessment of the dispersion requires information on the wind. As is well-known, Doppler weather radar is capable of providing wind data, but this possibility is not considered in the present work. Instead, the emphasis is laid on precipitation.

In addition to weather radar, direct or indirect information on the second component, the occurrence and strength of precipitation, is supplied by numerical weather predictions, surface-based observations and satellite imagery of clouds. Compared to these other sources of information, the most important benefit of using weather radar or, better still, a network of radars, is the coverage of a large area with high spatial and temporal resolution essentially in real time. Furthermore, because the scavenging coefficient Λ is related to the radar reflectivity factor Z , and the latter is closely associated with the

quantity measured by radar, the equivalent radar reflectivity factor Z_e , radar can be used to evaluate the third component, too, i.e., the efficiency of precipitation scavenging.

On the basis of Figs. 8-10, measured values of $\text{dB}Z_e$, when converted into $\text{dB}Z$, give a way of replying in round numbers to the question of the cleansing effect of precipitation and, in relative terms, to the question of the wet deposition. Furthermore, because of the analogy between the relationships of R and Λ to Z , the weather radar software usually used to create displays of precipitation rates and accumulated precipitation amounts can easily be modified to show distributions of Λ and its integrals in time. Such images can provide valuable information about the areas where a substantial portion of the pollutants is deposited onto the ground or, alternatively, remains airborne. Based on the movement of the precipitation areas, it is also possible to make short-term forecasts of those areas most likely to be exposed to wet deposition.

As an alternative to the $\Lambda - Z$ relation (3.8), one may apply the $\Lambda - R$ relation (3.7). A practical query is which of the two to favour. The stronger dependence of Λ on R than on Z (see Figs. 8-9) supports the use of the $\Lambda - R$ method. If, however, no additional precipitation data, such as rain gauge measurements, are available to improve the accuracy of radar-derived precipitation rates R , it is inefficient to make several successive conversions, first perhaps from Z_e to Z , then from Z to R and finally from R to Λ . In that case the $\Lambda - Z$ method is preferred.

In many cases, radar measurements are supplemented by some independent ground-level measurements of precipitation that are relatively accurate but have a limited spatial and temporal resolution. An adjustment of the radar-derived precipitation rate R to this data and subsequent use of the $\Lambda - R$ relation are likely to improve the accuracy of wet deposition estimates. Such an improvement is not self-evident, however, but depends primarily on two factors: the height of the radar beam with relation to the pollutants, and changes in precipitation between the radar beam aloft and ground level. This ensues from the fact that while in hydrological applications of radar measurements the emphasis is laid on the amount of water falling to the ground, in estimates of wet deposition the amount of pollutants deposited per unit area is of importance.

As an example, let us first assume that the radar measurement volume is uniformly filled with Rayleigh scatterers and occupies the same space as the majority of the pollutant, so that the hydrometeor population producing the radar signal is the same as that which is scavenging the pollutants (see Fig. 12). If evaporation of contaminated hydrometeors below the radar beam alters their size spectrum and concurrently releases pollutants into the air, the $\Lambda - Z$ method tends to overestimate the deposition to the ground in units of g or Bq per m^2 , while the $\Lambda - R$ method with a gauge-adjusted R presumably works better. Nevertheless, the contrary can be expected in the case of accretional or orographic

growth of precipitation below the joint layer of pollutants and radar measurements. Second, if the radar pulse volume is again uniformly filled with hydrometeors but overshoots the pollutants, and the precipitation has a vertical gradient, the best guess of wet deposition to the ground might lie somewhere between the estimates due to the two methods.

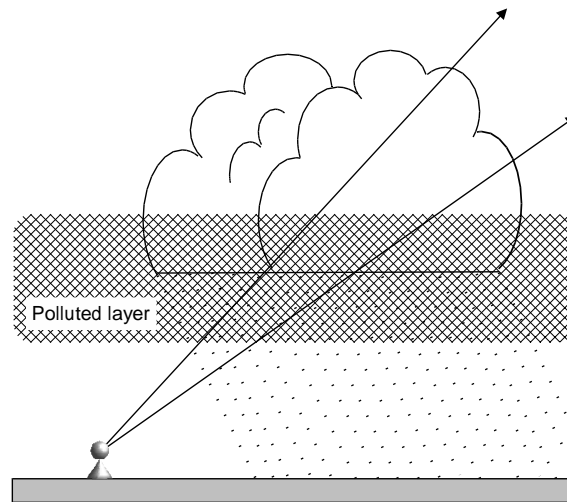


Fig. 12 *Schematic of the geometry of radar measurements in wet deposition estimates. Curvature of the Earth and the radar beam have been ignored.*

Unlike the situation assumed above, the radar pulse volume may be unevenly filled with hydrometeors because of, for example, partial beam overshooting of the precipitation. In addition to the beam overshooting and growth or evaporation of precipitation below the beam, sources of error in radar measurements for precipitation comprise variability of the phase and size distribution of hydrometeors (e.g., melting layer, large hail particles), beam-blocking by buildings and hills, anomalous propagation and attenuation of the beam, echoes from non-meteorological objects (e.g., ground and sea clutter near the radar, birds, insects) and radar calibration faults (see e.g., Joss and Waldvogel 1990; Sauvageot 1992, p. 152; Koistinen et al. 1999). Some of these sources of error can be rather easily identified on a radar display, and may even be automatically corrected in real time (e.g., Joss and Waldvogel 1990; Joss and Lee 1995; Harju and Puhakka 1980). The risks of the remaining error sources support carrying out of the gauge-adjustment of R (e.g., Koistinen and Puhakka 1981) or the vertical profile correction for Z (e.g., Koistinen 1991; Kitchen et al. 1994; Andrieu and Creutin 1995), or both, before estimates of Λ . Other potential techniques for rectifying radar data include differential reflectivity, dual-wavelength attenuation and multi-parameter methods (for a review, see Sauvageot 1992, p. 157-164).

Because variability of the phase and type of hydrometeors impairs radar observations and also affects the scavenging processes, one can expect that the greatest usefulness of radar in studies of wet deposition is obtained when the radar measurement volume coincides with the contaminated air layer and does not include the melting layer. In this case the number of possible error sources is at a minimum. On the other hand, since precipitation collects below-cloud aerosol particles and often also gas molecules far less effectively than it collects cloud droplets containing pollutants (Figs. 8-9), the height of the pollutants with relation to the cloud base has at least the same importance as their location relative to the radar beam and the melting layer. Obviously, the volume a cloud occupies does not coincide with the echoes observed by a conventional centimetre-wavelength weather radar, and it is not possible to observe the cloud base by radar when the precipitation is falling to the ground. Naturally, it is also impossible, using radar alone, to estimate the efficiency of in-cloud scavenging itself, i.e. the in-cloud scavenging factor F_{cl} . Instead, radar measurements of precipitation can be used to estimate the likelihood of in-cloud scavenged pollutants being removed from the atmosphere.

In addition to scientific research into precipitation scavenging, weather radar measurements can also be utilized in emergency situations. In order to be able to quantitatively predict amounts of wet deposition, estimates of airborne concentrations are additionally needed. These can be produced by a transport model for pollutants or by direct measurements by research flights, for example. On the other hand, the demonstration presented in Paper III and reviewed here in Sec. 4.2.2 indicated that even the original observations of Z_e alone, without any corrections for the error sources and hardly any information on the pollutants, may be very useful in pin-pointing the areas possibly contaminated by wet deposition. Because radar measures Z_e in real time, this can be of great help in a potential emergency situation during or immediately after an accidental release of harmful pollutants into the air. If the original, uncorrected observations of Z_e are the only ones available, it is important not to ignore the above-mentioned potential sources of error.

4.3.2 Remarks about the present studies

In this thesis, radar observations were used as input data for assessing wet deposition and for making empirical estimates of the $\Lambda - R$ relationships for radioactive and sulphur emissions. As regards the benefits and problems attached to the use of radar measurements, some differences can be found between the studies related to Chernobyl and to Inkoo.

In the Chernobyl-related studies for Southern Finland, in which the area of interest had a radius of about 200 km, the ability of radar to almost simultaneously monitor large

areas with a good spatial resolution was very essential. Because short-term precipitation amounts were not measured at the sites of the radioactivity monitoring stations, they had to be estimated. A sound way to do this was offered by radar measurements, with (Paper I) or without (Paper III) gauge-adjustment. Compared to the third possibility, i.e., the use of a network of precipitation gauges alone, more details of precipitation between the gauges could be observed. In addition to the good spatial resolution, the high temporal resolution of the radar measurements was also essential, even though no variation with time of the airborne concentrations was taken into account in assessing the wet deposition. The importance of the temporal resolution ensues from the fact that the scavenging coefficient Λ is basically proportional to the precipitation rate R , not to its time integral over a period of 12 or 24 hours, i.e., to the precipitation amount conventionally collected by gauges. In the studies related to the Inkoo power plant, the temporal resolution of radar measurements was probably even more important, as the modelled plume pattern varied somewhat in time. On the other hand, small-scale horizontal variations of R within 10 km of the power plants were smoothed out of the model input data. Only in a related report by Jylhä (1996) were they included.

Because some manual digitalizing was done in connection with both sets of radar data (Puhakka et al. 1990; Jylhä 1996), there was a risk of subjective bias. Nowadays, with the development of the automatic post-processing of radar data, this risk can be eliminated. Uncertainties in the Chernobyl-related radar data were additionally caused by beam overshooting at long ranges, as well as by echoes from insects, birds and ground clutter that interfered with the weak precipitation echoes near the radar. The radar data for the Inkoo power plant suffered most of all from beam-blocking by buildings near the radar and from partial beam overshooting. Owing to the gauge-adjustment of the radar data, it can be assumed, however, that these sources of error in radar measurements did not significantly affect the empirically derived $\Lambda - R$ relationships.

5 Summary

Precipitation scavenging of air pollutants includes in-cloud and below-cloud processes whereby pollutants become attached to liquid or solid hydrometeors, followed by the fall of the hydrometeors onto the ground as rain or snow. The scavenging coefficient Λ (s^{-1}) gives the fractional depletion rate of the pollutant concentration in air due to precipitation. The relationships discussed in this thesis between it, the precipitation rate R (mm h^{-1}) and the radar reflectivity factor Z ($\text{mm}^6 \text{m}^{-3}$) are based on the fact that they are all functions of the hydrometeor size spectrum. By assuming an exponential form for this spectrum and making some other simplifications, it can be shown theoretically that the dependencies between Λ , R and Z have the approximate power-law forms of $\Lambda \approx aR^b$ and $\Lambda \approx \alpha Z^\beta$. Many experimental studies also support the former relation, while very few have been previously published concerning the latter dependence. On the other hand, there are no general $\Lambda - R$ and $\Lambda - Z$ relationships; these vary, depending on the properties of the precipitation and pollutants. In the present thesis, the theoretical bases of the $\Lambda - R$ and $\Lambda - Z$ relations were deliberated and a few estimates for them were presented on the ground of theoretical and experimental work.

In the experimental studies, it was not possible to distinguish either between in-cloud and below-cloud scavenging or between the two stages in in-cloud scavenging, i.e., the transfer of pollutants into cloud droplets and the capture of these contaminated cloud droplets by precipitation particles. Hence the resulting scavenging coefficients described the net effect of all these processes. In theoretical considerations, however, a separation was made between the below-cloud scavenging coefficient, the in-cloud scavenging factor and the scavenging coefficient for pollutants inside cloud droplets, or, in other words, for contaminated cloud droplets.

In Paper I, radioactivity and precipitation measurements in Southern Finland after the Chernobyl accident were combined to produce empirical $\Lambda - R$ relationships for the particle-bound radionuclides involved. The average scavenging coefficient for the nuclides, weighted by the high-altitude nuclide concentrations, was found to be $\Lambda = (8 \mp 2) \cdot 10^{-5} \text{ s}^{-1} R^{0.65 \mp 0.2}$. The relation parameterised the total effect of in-cloud and below-cloud wet removal caused by hydrometeors mostly in the liquid phase. Even though several assumptions were needed, the result is in good agreement with earlier studies for sulphate and nitrate particles. It is also supported by a comparison of observed and calculated gamma radiation dose rates in ground-level air: the percentage of calculations that agreed with observations to within a factor of two was 76%, and there was a significant positive correlation between them, with a logarithmic correlation coefficient of 0.66.

A similar correlation coefficient was found in Paper III where the observed doses were merely compared with time integrals of Λ , a quantity approximately proportional to the accumulated wet deposition. The scavenging coefficient was this time reckoned directly from observations of the radar reflectivity factor using a $\Lambda - Z$ dependence for contaminated cloud droplets. On the basis of the theoretical considerations in Paper II, the dependence was taken to be $\Lambda = 1.5 \cdot 10^{-5} \text{ s}^{-1} Z^{0.53}$ in the case of moderate to heavy rain and slightly steeper in the case of very weak rain. For in-cloud pollutants, as well as for below-cloud submicron aerosol particles and highly soluble gases, the theoretical results of Paper II imply that in rain an increase in the radar reflectivity factor of 10 dbZ approximately corresponds to a two- to fourfold increase in Λ . This results in turn in a similar increase in the deposition flux and in an analogous decrease in the residence times of pollutants in the atmosphere. In snowfall, the dependence of Λ on Z is probably somewhat weaker than in rain, but is also more uncertain due to the large variety of types and shapes of solid hydrometeors.

An uppermost estimate for the $\Lambda - R$ relation of freshly-emitted sulphur species in snowfall arose from a wintertime case study carried out near a coal-fired power plant at Inkoo on the south coast of Finland (Papers IV and V). By comparing deposition sampling results with the output of a short-range deposition model, it was inferred that $\Lambda \leq 10^{-6} \text{ s}^{-1} R^{0.7}$ for sulphur emissions in wet snowfall within the first 10 km of the source. This means that the percentage of emitted sulphur being scavenged within the study area was equal to or less than about 0.7%, which is in agreement with previous experimental studies around point sources. Although sulphate concentrations in the deposition samples did not reveal any discernible increase downwind of the power station, it is possible that precipitation scavenging of plume-related sulphur and hydrochloride, in particular, added to the acidity in the vicinity of the source but in an area which lay between the collectors. On the other hand, effects of alkaline fly ash on the acidity presumably remained minor.

The model estimates related to the Inkoo experiment illustrate the importance of taking into account the wind drift of precipitation particles through the plume. Because the fall trajectories are out of the vertical, it is unlikely that the wet-deposited amounts of primary pollutants on the ground would decrease monotonously with increasing distance from the chimney. Instead, the maximum wet deposition area may be located at a distance of 1-5 km from the source, for example, the exact value depending on the fall speed of the hydrometeors compared with the wind speed and on the plume height. It is worth keeping this feature in mind in high-resolution studies of precipitation scavenging of pollutants, not only in snowfall but also in rainfall.

Of special importance in this thesis were the measurements of precipitation by weather radar. As demonstrated here, they can be utilised in scientific experiments by which distributions of wet deposition are assessed and scavenging parameterisations are developed and verified. Moreover, because weather radar estimates the spatial distribution of the radar reflectivity factor Z essentially in real time, and because Λ is correlated with Z , a network of radars may form an important part of a real-time monitoring and warning system that can be immediately effective in the event of an accidental release of hazardous materials into the air. The problems attending the use of radar in precipitation scavenging estimates are mainly related to the uncertain characteristics and dispersion heights of the pollutants and to the well-known error sources in weather radar measurements of precipitation. A vertical profile correction of Z and an adjustment of radar-derived precipitation rate R to some independent ground-level measurements of precipitation and a subsequent use of the $\Lambda - R$ relation are both likely to improve the accuracy of wet deposition estimates. As suggested by the Chernobyl case study, however, even original radar observations alone, without any corrections for the error sources and hardly any information on the pollutants, may be very useful in pinpointing the areas possibly contaminated by wet deposition.

Acknowledgements

The seed for this thesis was already sown at the beginning of 1986, when I started to study, as an undergraduate student, the use of weather radar in air pollution estimates. A few months later "Tuulia", the two-year old Doppler weather radar of the University of Helsinki, made measurements of radioactive rain over Southern Finland. The fourth reactor of the Chernobyl nuclear power plant had exploded, resulting in the largest civil nuclear catastrophe by far.

I wish to commemorate those who died in the disaster and to express our condolences to the children and adults suffering from its consequences in the Ukraine, Belarus and other neighboring countries. The work of all those who endeavour to ensure, in various different ways, that "another Chernobyl" will never occur, is highly appreciated.

The work on which this thesis is based was performed at the Department of Meteorology in the University of Helsinki and was completed in the Air Quality Research and Meteorological Research Divisions of the Finnish Meteorological Institute.

The greatest debt I owe to Prof. Timo Puhakka, who has taught me much of the radar meteorology and cloud physics presented here and, as the supervisor of my graduate studies and thesis, encouraged me incessantly and made constructive comments on my

work. Prof. Hannu Savijärvi, the other preliminary inspector of this thesis, and Emeritus Prof. Eero Holopainen are also gratefully acknowledged for their continuous support.

The experimental parts of this thesis would not have been possible without the generous help of my colleagues at the Department of Meteorology as well as the activities of numerous people at Imatran Voima Oy, the Ministry of the Interior, the Finnish Defence Forces, and the Finnish Centre for Radiation and Nuclear Safety. I am deeply indebted to you all. In particular, Mr. Matti Leskinen is thanked for his manifold advice on the analysis of radar measurements, and Mr. Jarmo Koistinen is thanked for guiding me in the early stages of my scientific career.

Sincere thanks are extended to the unknown reviewers of Papers I-V who pored over the manuscripts and helped to improve them. Thanks are also due to Mr. Robin King for correcting the language of every part of this thesis and for his professional comments.

Gratitude is gladly expressed to my current employer, the Finnish Meteorological Institute. Professors Erkki Jatila, Göran Nordlund, Mikko Alestalo, Sylvain Joffre and Juhani Rinne, as well as many staff members are kindly acknowledged for their support and for providing me with good working conditions.

The early phases of this work were financed in part by the Maj and Tor Nessling Foundation; Imatran Voima Oy; the Academy of Finland; the Jenny and Antti Wihuri Foundation; the Vilho, Yrjö, and Kalle Väisälä Foundation; the Aili Nurminen Foundation; and the Kone Foundation. All these bodies are cordially thanked.

Finally, I wish to lovingly thank those in my private life for their encouragement and help during the course of this Ph.D. work. My friends, parents, brother and sisters all contributed to its fulfilment in one way or another. I am grateful to you all. My warmest thanks I express to my daughter Mirva and son Miikka for their patience and joy of life, and for giving me so many things to concentrate on and to enjoy.

References

- Alheit, R. R., A. I. Flossmann, and H. R. Pruppacher, 1990: A theoretical study of the wet removal of atmospheric pollutants. Part IV: The uptake and redistribution of aerosol particles through nucleation and impaction scavenging by growing cloud drops and ice particles. *J. Atmos. Sci.*, **47**, 870–887.
- Andrieu, H., and J. D. Creutin, 1995: Identification of vertical profiles of radar reflectivity for hydrological applications using an inverse method: Part I: Formulation. *J. Appl. Meteor.*, **34**, 225–239.
- Appleby, L. J., 1998: Overview of the proceedings and papers of the NATO/SCOPE-RADTEST advanced research workshop in Vienna. *Atmospheric nuclear tests*, C. S. Shapiro, Ed., NATO ASI Series, 2. Environment, Vol. 2, 9–60.
- ApSimon, H. M., K. L. Simms, and Collier, C. G., 1988: The use of weather radar in assessing deposition of radioactivity from Chernobyl across England and Wales. *Atmos. Environ.*, **22**, 1895–1900.
- Arvela, H., M. Markkanen, and H. Lemmelä, 1990: Mobile survey of environmental gamma radiation and fall-out levels in Finland after the Chernobyl accident. *Radiat. Prot. Dosimet.*, **32**, 177–184.
- Asman, W. A. H., 1995: Parameterization of below-cloud scavenging of highly soluble gases under convective conditions. *Atmos. Environ.*, **29**, 1359–1368.
- BASYS, 2000: Baltic Sea system study: Final report. [Available online at http://www.io-warnemuende.de/Projects/Basys/reports/final/en_home.htm]
- Beard, K. V., and H. T. Ochs, 1984: Collection and coalescence efficiencies for accretion. *J. Geophys. Res.*, **89**, 7165–7169.
- Beard, K. V., and R. M. Rauber, 1990: Cloud microphysics and radar: panel report. *Radar in meteorology: Battan memorial and 40th anniversary radar meteorology conference*, D. Atlas, Ed., Amer. Meteor. Soc., 341–347.
- Berge, E., J. Bartnicki, K. Olendrzynski, and S. G. Tsyro, 1999: Long-term trends in emissions and transboundary transport of acidifying air pollution in Europe. *J. Environ. Manage.*, **57**, 31–50.
- Chamberlain, A. C., 1959: Deposition of iodine-131 in Northern England in October 1957. *Quart. J. R. Met.*, **85**, 350–361.
- Chang, T. Y., 1984: Rain and snow scavenging of HNO₃ vapor in the atmosphere. *Atmos. Environ.*, **18**, 191–197.
- Chang, T. Y., 1986: Estimates of nitrate formation in rain and snow systems. *J. Geophys. Res.*, **91**, 2805–2818.
- Clark, M. J., and F. B. Smith, 1988: Wet and dry deposition of Chernobyl releases, *Nature*, **332**, 245–249.

- Collier, C. G., 1999: Weather radar development in Europe post COST-73. Preprints, *29th Int. Conf. on Radar Meteor.*, Montreal, Amer. Meteor. Soc., 1-4.
- Diehl, K., S. K. Mitra, and H. R. Pruppacher, 1995: A laboratory study of the uptake of HNO₃ and HCl vapor by snow crystals and ice spheres at temperatures between 0 and -40°C. *Atmos. Environ.*, **29**, 975-981.
- Diehl, K., S. K. Mitra, and H. R. Pruppacher, 1998: A laboratory study on the uptake of HCl, HNO₃, and SO₂ gas by ice crystals and the effect of these gases on the evaporation rate of the crystals. *Atmos. Res.*, **47-48**, 235-244.
- Dvonch, J. T., J. R. Graney, F. J. Marsik, G. J. Keeler, and R. K. Stevens, 1998: An investigation of source-receptor relationships for mercury in south Florida using event precipitation data. *Sci. Total Environ.*, **213**, 95-108.
- Eichel, C., M. Kramer, L. Schutz, and S. Wurzler, 1996: The water-soluble fraction of atmospheric aerosol particles and its influence on cloud microphysics. *J. Geophys. Res.*, **101**, D29499-29510.
- Engelmann, R. J., 1968: The calculation of precipitation scavenging. *Meteorology and atomic energy 1968*, D.H. Slade, Ed., U.S. Atomic Energy Commission, 208-221.
- EPA, 2000: *National air quality and emissions trends report, 1998*. U.S. Environmental Protection Agency, Office of Air Quality Planning and Standards, Research Triangle Park, NC 27711, April 2000. [Available online at <http://www.epa.gov/oar/aqtrnd98/>].
- Erlandsson, B., and M. Isaksson, 1988: Relation between the air activity and the deposition of Chernobyl debris. *Environ. Int.*, **14**, 165-175.
- Feingold, G., and Z. Levin, 1987: Lognormal fit to raindrop spectra from frontal convective clouds in Israel. *J. Climate Appl. Meteor.*, **25**, 1346-1363.
- Galloway, J. N., 1995: Acid deposition: perspectives in time and space. *Water, Air, Soil Pollut.*, **85**, 15-24.
- Goddard, D. M., and B. J. Conway, 1990: Near-real-time precipitation analysis over Europe. *Weather radar networking: seminar on COST Project 73*, C. G. Collier and M. Chapuis, Eds., Kluwer, 330-338.
- González, A.J., 1996: Chernobyl - Ten years after. IAEA Bulletin, Vol. 38/3, p. 2-13. [Available online at <http://www.iaea.or.at/worldatom/inforesource/bulletin/bull383/>]
- Harju, A., and T. Puhakka, 1980: A method of correcting quantitative radar measurements for partial beam blocking. Preprints, *19th Conf. on Radar Meteor.*, Boston, Amer. Meteor. Soc., 234-239.
- Hinds, W. C., 1982: *Aerosol technology: properties, behavior, and measurement of airborne particles*. Wiley & Sons, New York. 424 pp.

- Hirose, K., S. Takatani, and M. Aoyama, 1993: Wet deposition of radionuclides derived from the Chernobyl accident. *J. Atmos. Chem.* **17**, 61–71.
- IAEA, cited 2000: Nuclear Power Status 1999. IAEA Press Centre, 6 March 2000, revised 25 April 2000. [Available online at http://www.iaea.org/worldatom/Press/P_release/2000/prn0900.html.]
- IEA, 1998: Key world energy statistics from the IEA. International Energy Agency, Paris, France, November 1998. [Available online at http://www.iea.org/stats/files/keystats/stats_98.htm]
- Ilus, E., K.-L. Sjöblom, H. Aaltonen, and H. Arvela, 1987: Monitoring of radioactivity in the environs of Finnish nuclear power stations in 1986. *Report STUK-A67*, Finnish Centre for Radiation and Nuclear Safety, Helsinki, Finland, 82 pp.
- IPCC, 2000: Special Report on Emissions Scenarios. Summary for Policymakers. A special report of Working Group III of the Intergovernmental Panel on Climate Change. May, 2000. [Available online at <http://www.ipcc.ch/>]
- Joss, J., and R. Lee, 1995: The application of radar-gauge comparison to operational precipitation profile corrections. *J. Appl. Meteor.*, **34**, 2612–2630.
- Joss, J., and A. Waldvogel, 1990: Precipitation measurement and hydrology. *Radar in meteorology: Battan memorial and 40th anniversary radar meteorology conference*, D. Atlas, Ed., Amer. Meteor. Soc., 577–606.
- Jost, D. T., H. W. Gäggeler, U. Baltensperger, B. Zinder, and P. Haller, 1986: Chernobyl fallout in size-fractionated aerosol. *Nature*, **324**, 22–23.
- Jylhä, K., 1989: Lähi- ja kaukolaskeuman märän komponentin erottamismahdollisuudet mittauksen avulla. Technical Report No. 5, Department of Meteorology, Univ. of Helsinki, ISBN 951-45-4926-0. 36 pp. (Abstract in English)
- Jylhä, K., 1990: Precipitation scavenging of radioactive substances released from the Chernobyl power plant. Report No. 38, Department of Meteorology, Univ. of Helsinki, Finland, 32 pp.
- Jylhä, K., 1996: Wet deposition near the Inkoo power station during a wintertime experiment. Report No. 44, Department of Meteorology, Univ. of Helsinki, Finland, 89 pp.
- Jylhä, K., P. Saarikivi, J. Koistinen, and T. Puhakka, 1986: Esitutkimus Dopplersäätutkan käyttömahdollisuuksista Loviisan ja Inkoon lähileviämisarvioinneissa. Imatran Voima Oy, T&K-Tiedotteita, IVO-B-07/86, Helsinki, ISBN 951-9100-52-0. 87 pp. (Abstract in English)
- Kasper-Giebl, A., M. F. Kalina, and H. Puxbaum, 1999: Scavenging ratios for sulfate, ammonium and nitrate determined at Mt. Sonnblick (3106 m a.s.l.). *Atmos. Environ.*, **36**, 895–906.

- Kauppinen, E. I., and T. A. Pakkanen, 1990: Coal combustion aerosols: a field study. *Environ. Sci. Technol.*, **24**, 1811–1818.
- Kauppinen, E. I., R. E. Hillamo, S. H. Aaltonen, and K. T. S. Sinkko, 1986: Radioactivity size distributions of ambient aerosols in Helsinki, Finland, during May 1996 after the Chernobyl accident: preliminary report. *Environ. Sci. Technol.*, **20**, 1257–1259.
- Kitchen, M., R. Brown, and A. G. Davies, 1994: Real-time correction of weather radar data for the effects of bright band, range and orographic growth in widespread precipitation. *Q. J. R. Meteorol. Soc.*, **120**, 1231–1254.
- Koistinen, J., 1991: Operational correction of radar rainfall errors due to the vertical reflectivity profile. Preprints, *25th Int. Conf. on Radar Meteor.*, Paris, Amer. Meteor. Soc., 91–94.
- Koistinen, J., and T. Puhakka, 1981: An improved spatial gage-radar adjustment technique. Preprints, *20th Int. Conf. on Radar Meteor.*, Boston, Amer. Meteor. Soc., 179–186.
- Koistinen, J., R. King, E. Saltikoff, and A. Harju, 1999: Monitoring and assessment of systematic measurement errors in the NORDRAD network. Preprints, *29th Int. Conf. on Radar Meteor.*, Montreal, Amer. Meteor. Soc., 765–768.
- Korhonen, P., M. Kulmala, H.-C. Hansson, I. B. Svenningsson, and N. Rusko, 1996: Hygroscopicity of pre-existing particle distribution and formation of cloud droplets: a model study. *Atmos. Res.*, **41**, 249–266.
- Laaksonen, A., P. Korhonen, M. Kulmala, and R. J. Charlson, 1998: Modification of the Köhler equation to include soluble trace gases and slightly soluble substances. *J. Atmos. Sci.*, **55**, 853–862.
- Langner, J., L. Robertson, C. Persson, and A. Ullerstig, 1998: Validation of the operational emergency response model at the Swedish Meteorological and Hydrological Institute using data from ETEX and the Chernobyl accident. *Atmos. Environ.*, **32**, 4325–4333.
- Makhon'ko, K. P., and S. G. Malakhov, 1967: Results of systematic observations of hot particles in the surface layer in the Moscow area from 1961–1963. *Radioactive isotopes in the atmosphere and their use in meteorology*, Karol, I.L., Kirichenko, L. V., Krasnopevtsev, Yu. V., Kurganskaya, V. M., Malakhov, S. G., Sereda, G. A., and Yagodovskii, I. V., Eds., Moskva 1965 (in Russian), Jerusalem 1967 (in English), 141–150.
- Marshall, J. S. and W. M. Palmer, 1948: The distribution of raindrops with size. *J. Meteor.*, **5**, 165–166.
- Martin, J. J., P. K. Wang, and H. R. Pruppacher, 1980: A theoretical determination of the efficiency with which aerosol particles are collected by simple ice crystal plates. *J. Atmos. Sci.*, **37**, 1628–1663.

- McMahon, T. A., and P. J. Denison, 1978: Empirical atmospheric deposition parameters – a survey. *Atmos. Environ.*, **13**, 571–585.
- Miller, N. L., and P. K. Wang, 1989: Theoretical determination of the efficiency of aerosol particle collection by falling columnar ice crystals. *J. Atmos. Sci.*, **46**, 1656–1663.
- Mitra, S. K., U. Barth, and H. R. Pruppacher, 1990a: A laboratory study of the efficiency with which aerosol particles are scavenged by snow flakes. *Atmos. Environ.*, **24A**, 1247–1254.
- Mitra, S. K., U. Barth, and H. R. Pruppacher, 1990b: A laboratory study on the scavenging of SO₂ by snow crystals. *Atmos. Environ.*, **24A**, 2307–2312.
- Murakami, M., C. Magono, and K. Kikuchi, 1985: Experiments on aerosol scavenging by natural snow crystals. Part III: The effect of snow crystal charge on collection efficiency. *J. Meteor. Soc. Japan*, **63**, 1127–1137.
- Nordlund, G., and H. Tuomenvirta, 1998: Spatial variation in wet deposition amounts of sulphate due to stochastic variations in precipitation amounts. *Atmos. Environ.*, **32**, 2913–2921.
- Okita, T., H. Hara, and N. Fukuzaki, 1996: Measurements of atmospheric SO₂ and SO₄²⁻, and determination of the wet scavenging coefficient of sulfate aerosols for the winter monsoon season over the Sea of Japan. *Atmos. Environ.*, **30**, 3733–3739.
- Paatero, J., 2000: Deposition of Chernobyl-derived transuranium nuclides and short-lived radon-222 progeny in Finland. Finnish Meteorological Institute Contributions, No. 28, Finnish Meteorological Institute, Helsinki, Finland, 128 pp.
- Park, S.-U., H.-J. In, and Y.-H. Lee, 1999: Parameterization of wet deposition of sulfate by precipitation rate. *Atmos. Environ.*, **33**, 4469–4475.
- Persson, C., H. Rodhe, and L.-E. De Geer, 1987: The Chernobyl accident – A meteorological analysis of how radionuclides reached and were deposited in Sweden. *Ambio*, **16**, 20–31.
- Pruppacher, H. R., and J. D. Klett, 1997: *Microphysics of clouds and precipitation*. 2nd ed. Kluwer, 954 pp.
- Puhakka, T., K. Jylhä, P. Saarikivi, J. Koistinen, and J. Koivukoski, 1988: Meteorological factors influencing the radioactive deposition in Finland after the Chernobyl accident. Report No. 29, Department of Meteorology, Univ. of Helsinki, Finland, 49 pp.
- Puhakka, T., K. Jylhä, P. Saarikivi, J. Koistinen, and J. Koivukoski, 1990: Meteorological factors influencing the radioactive deposition in Finland after the Chernobyl accident. *J. Appl. Meteor.*, **29**, 813–829.
- Respondek, P. S., R. R. Alheit and H. R. Pruppacher, 1995: A theoretical study of the wet removal of atmospheric pollutants. Part V: The uptake, redistribution, and deposition of (NH₄)₂SO₄ by a convective cloud containing ice. *J. Atmos. Sci.*, **52**, 2121–2132.

- Rodhe, H., P. Grennfelt, J. Wisniewski, C. Ågren, G. Bengtsson, K. Johansson, P. Kauppi, V. Kucera, L. Rasmussen, B. Rosseland, L. Schotte, and G. Selldén, 1995: Acid Reign '95? – Conference summary statement. *Water, Air, Soil Pollut.*, **85**, 1–14.
- Roeckner, E., L. Bengtsson, J. Feichter, J. Lelieveld, and H. Rodhe, 1999: Transient climate change simulations with a coupled atmosphere-ocean GCM including the tropospheric sulfur cycle. *J. Climate*, **12**, 3004–3032.
- Saltbones, J., A. Foss, and J. Bartnicki, 1998: Norwegian Meteorological Institute's real-time dispersion model SNAP (Severe Nuclear Accident Program): Runs for ETEX and ATMES II experiments with different meteorological input. *Atmos. Environ.*, **32**, 4277–4283.
- Sauter, D. P., and P. K. Wang, 1989: An experimental study of the scavenging of aerosol particles by natural snow crystals. *J. Atmos. Sci.*, **46**, 1650–1655.
- Sauvageot, H., 1992: *Radar meteorology*. Artech House, 366 pp.
- Savchenko, K. V., 1995: *The ecology of the Chernobyl catastrophe: scientific outlines of an international programme of collaborative research*. Man and the biosphere series, Vol. 16, Unesco & The Parthenon Publishing Group, 200 p.
- Savolainen, A. L., T. Hopekoski, J. Kilpinen, P. Kukkonen, A. Kulmala, and I. Valkama, 1986: Dispersion of radioactive releases following the Chernobyl nuclear power plant accident. Interim report No. 1986:2, Finnish Meteorological Institute, Helsinki, Finland, 44 pp.
- Savolainen, A. L., K. Leminen, B. Tammelin, A. Lange, O. Kemppi, and R. King, 1991: Ydinvoimalaitoksiin liittyvien meteorologisten mittausjärjestelmien perus selvitys. Rep. STUK–YTO–TR 25, Finnish Centre for Radiation and Nuclear Safety, Helsinki, ISSN 0785–9325, 60 pp. (In Finnish)
- Saxén, R., T. K. Taipale, and H. Aaltonen, H., 1987: Radioactivity of wet and dry deposition and soil in Finland after the Chernobyl accident in 1986. *Report STUK–A57*, Finnish Centre for Radiation and Nuclear Safety, Helsinki, Finland, 44 pp.
- Scott, B. C., 1982: Theoretical estimates of the scavenging coefficient for soluble aerosol particles as a function of precipitation type, rate and altitude. *Atmos. Environ.*, **16**, 1753–1762.
- Seinfeld, J. H., and S. N. Pandis, 1998: *Atmospheric chemistry and physics: from air pollution to climate change*. Wiley & Sons, 1326 pp.
- Sekhon, R. S., and R. C. Srivastava, 1970: Snow size spectra and radar reflectivity. *J. Atmos. Sci.*, **27**, 299–307.
- Seliga, T. A., H. Direskeneli, and K. Aydin, 1989: Potential role of differential reflectivity to estimate scavenging of aerosols. Preprints, *24th Conf. on Radar Meteorology*, Tallahassee, Florida, Amer. Meteor. Soc., 363–366.

- Sinkko, K., H. Aaltonen, R. Mustonen, T. K. Taipale, and J. Juutilainen, 1987: Airborne radioactivity in Finland after the Chernobyl accident in 1986. *Report STUK-A56*, Finnish Centre for Radiation and Nuclear Safety, Helsinki, Finland, 42 pp.
- Skolnik, M. I., 1962: *Introduction to radar systems*. McGraw-Hill, New York. 648 pp.
- Slinn, W. G. N., 1977: Some approximations for the wet and dry removal of particles and gases from the atmosphere. *Water, Air, Soil Pollut.*, **7**, 513–543.
- Smith, F. B., 1981: Probability prediction of the wet deposition of airborne pollution. *Air pollution modeling and its application I*, C. De Wispelaere, Ed., Plenum Press, 67–98.
- Smith, P. L., 1984: Equivalent radar reflectivity factors for snow and ice particles. *J. Climate Appl. Meteor.*, **23**, 1258–1260.
- Sparmacher, H., K. Fulber, and H. Bonka, 1993: Below-cloud scavenging of aerosol particles: Particle-bound radionuclides – experimental. *Atmos. Environ.*, **27A**, 605–618.
- Streets, D. G., G. R. Carmichael, M. Amann, and R. L. Arndt, 1999: Energy consumption and acid deposition in Northeast Asia. *Ambio*, **28**, 135–143.
- Toon, O. B., 2000: How pollution suppresses rain. *Science*, **287**, 1763–1765.
- Ulbrich, C. W., 1983: Natural variations in the analytical form of the raindrop-size distribution. *J. Climate Appl. Meteor.*, **24**, 1764–1775.
- Valdez, M. P., G. A. Dawson, and R. C. Bales, 1989: Sulfur dioxide incorporation into ice depositing from the vapor. *J. Geophys. Res.*, **94**, 1095–1103.
- van Aardenne, J. A., G. R. Carmichael, H. II Levy, D. Streets, and L. Hordijk, 1999: Anthropogenic NO_x emissions in Asia in the period 1990–2020. *Atmos. Environ.*, **33**, 633–646.
- Wang, P. K., and H. R. Pruppacher, 1977: An experimental determination of the efficiency with which aerosol particles are collected by water drops in subsaturated air. *J. Atmos. Sci.*, **34**, 1664–1669.
- Wang, P. K., and H. Lin, 1995: Comparison of model results of collection efficiency of aerosol particles by individual water droplets and ice crystals in a subsaturated atmosphere. *Atmos. Res.*, **38**, 381–390.
- Wang, P. K., and W. Ji, 1997: Numerical simulation of three-dimensional unsteady flow past ice crystals. *J. Atmos. Sci.*, **54**, 2261–2274.
- Weiss, W., 1997: Strategies for monitoring and for the assessment of the radiological situation in an emergency. *Radiat. Prot. Dosimet.*, **73**, 7–10.
- Wernli, C., 1987: Radiological consequences of the Chernobyl accident for Switzerland. *Radiat. Prot. Dosimet.*, **19**, 235–238.
- Wurzler, S., A. I. Flossmann, H. R. Pruppacher, and S. E. Schwartz, 1995: The scavenging of nitrate by clouds and precipitation. *J. Atmos. Chem.*, **20**, 259–280.

Appendix A

Corrections to Papers I and II

Paper I (Jylhä 1991)

Table 1 on page 266:

OLX** *should be* OLK**

|| From 15 April to be exact, but in practice from about 1200 UTC on 27 April to 0930 UTC on 30 April 1986.

should be:

|| From 15 April to be exact, but in practice from about 1200 UTC on 27 April to 0700 UTC on 30 April 1986.

¶ From 1 April to be exact, but in practice from about 1200 UTC on 27 April to 0930 UTC on 30 April 1986.

Paper II (Jylhä 1999a)

Table 1 on page 1422:

Intercept N_0 (m^{-4}) 8×10^6 Eqs. (14a, 14c)

Slope λ Eq. (13) Eqs. (14b, 14c)

should be:

Intercept N_0 (m^{-4}) 8×10^6 Eqs. (12a, 12c)

Slope λ Eq. (11) Eqs. (12b, 12c)

Page 1425, below Eq. (12c):

Combining (14a) and (14b) with (14c)

should be:

Combining (12a) and (12b) with (12c)

Fig. D1a in Appendix D on page 1432:

Legend: κ_{g1} *should be* κ_{g2}

κ_{g2} *should be* κ_n

κ_n *should be* κ_{g1}

Fig. D1b in Appendix D on page 1432:

Legend: κ_{g1} *should be* $\kappa_{g2(1-2)}$

$\kappa_{g2(1-2)}$ *should be* $\kappa_n(1-2)$

$\kappa_n(1-2)$ *should be* κ_{g1}